REGISTERED NO. M. 3121

EP 24 1951
PHYSICS LIBRARY

PROCEEDINGS
OF THE
INDIAN ACADEMY
OF SCIENCES

VOL. XXXIII] *SECTION A* [NO. 5

MAY, 1951

Price Rs. 2 or 3 Sh. *Annual Subscription Rs. 18*

PRINTED AT THE BANGALORE PRESS, BANGALORE CITY, BY G. SRINIVASA RAO,
SUPERINTENDENT, AND PUBLISHED BY THE INDIAN ACADEMY OF SCIENCES,
BANGALORE.

ELASTIC CONSTANTS OF BARYTES AND CELESTITE

By T. Seshagiri Rao

(*From the Physical Laboratories, Osmania University, Hyderabad-Dn.*)

Received March 2, 1951

(Communicated by Prof. S. Bhagavantam, F.A.SC.)

1. Introduction

Barytes and celestite, sulphates of barium and strontium respectively, belong to the orthorhombic system with V_h^{16} as the space group. The elastic constants of barytes have been determined by Voigt (1938) and by Bergmann (1938). Those of celestite have not so far been determined. In an attempt to study the elastic properties by the wedge method of single crystals belonging to the same isomorphous series, the elastic constants of the sulphates of barium and strontium have been determined by the author.

2. The Elastic Constants of an Orthorhombic Crystal

The orthorhombic system is characterised by nine constants C_{11},C_{22}, C_{33}, C_{44}, C_{55}, C_{66}, C_{12}, C_{23} and C_{13}. The *a*-, *b*-, *c*-crystallographic axes are respectively taken as the X_1-, X_2-, X_3-axes. To get all the nine constants, at least six sections with different orientations are required. Six of the nine constants of the type C_{ii} come out directly from the axial cuts, using the secular Christoffel determinant. Thus a plate whose normal coincides with the *a*-axis (called the X_1-cut) gives C_{11}, C_{55} and C_{66}; the X_2-cut gives C_{22} C_{44} and C_{66} and the X_3-cut yields C_{33}, C_{44} and C_{55} giving the six constants C_{ii} with three checks. The remaining three constants C_{12}, C_{23} and C_{13} are determined by using suitable oblique cuts. For these cuts, however, a method which obviates the necessity of using approximate solutions is adopted. This method is just the same as the one given by Sundara Rao (1950) and hence only the essential equations are given below omitting the details.

Taking the X_1 45 X_2 cut (the cut whose normal is perpendicular to the X_1-axis and is inclined at 45° to X_2 and X_3 and so on), the value of C_{23} is obtained from the relation

$$C_{23} = \pm \sqrt{[\{2x_1 - (C_{33}' + C_{44}')\}^2 - 4\,C_{34}'^2]} - C_{44}$$

where x_1 is the longitudinal frequency of the particular section which can be experimentally determined. The rest of the quantities are previously determined, $C_{33}' + C_{44}'$ being equal to $\frac{1}{2}$ $(C_{22} + C_{33} + 2C_{44})$ and $4C_{34}' = (C_{33} - C_{22})$.

The ambiguity in the sign of the radical can, however, be decided easily since in the limiting case when $C_{34}' \to 0$ the value of C_{23} should be that obtained by putting $x_1 = C_{33}'$, where $C_{33}' = \frac{1}{4}(C_{22} + C_{33} + 2C_{23} + 4C_{44})$ and whichever value of C_{23} is nearer the approximate one is taken as the correct one.

In a similar manner, the other constants C_{13} and C_{12} are determined from $X_2\,45\,X_3$ and $X_3\,45\,X_1$ cuts using the relations given below:

$X_2\,45\,X_3$ cut:

$$C_{13} = \pm \sqrt{[\{2x_1 - (C_{33}' + C_{44}')\}^2 - 4C_{34}'^2]} - C_{55}$$

where $C_{33}' + C_{44}' = \frac{1}{2}(C_{11} + C_{33} + 2C_{55})$

and $4C_{34}' = (C_{33} - C_{11})$.

In the limiting case, $x_1 = C'_{33} = \frac{1}{4}(C_{11} + C_{33} + 2C_{13} + 4C_{55})$.

$X_3\,45\,X_1$ cut:

$$C_{12} = \pm \sqrt{[\{2x_1 - (C_{33}' + C_{44}')\}^2 - 4C_{34}'^2]} - C_{66}$$

where $C_{33}' + C_{44}' = \frac{1}{2}(C_{11} + C_{22} + 2C_{66})$

and $4_{34}' = (C_{11} - C_{22})$.

In the limiting case, $x_1 = C_{33}' = \frac{1}{4}(C_{11} + C_{22} + 2C_{12} + 4C_{66})$.

3. *Experimental Technique*

The crystal faces and axes are identified by using the crystallographic data given by Dana (1947). In the case of barytes the *c*-axis is easily identified being perpendicular to the prominent tabular face (001). The other two orthogonal axes *a*- and *b*- are located by examining the crystal between crossed polaroids. In the case of celestite, the faces are identified by measuring the interfacial angles with a contact goniometer. Both the crystals have an easy cleavage perpendicular to the *c*-axis and the X_3-cuts are obtained by tapping the crystals with a sharp edge.

All the six sections for each crystal are cut and ground to uniform thickness by hand and the different orientations are correct to within 1°. Wherever possible, more than one section of different thicknesses have been worked. The ultrasonic velocities in the crystal plates are determined by using the wedge method developed by Bhagavantam and Bhimasenachar (1944). Ultrasonic frequencies upto 12 Mc/Sec are used. The frequencies are determined by a precision heterodyne wavemeter which is capable of giving an accuracy of 1 part in 50,000.

4. *Experimental Data and Results*

The experimental data obtained and tne results calculated are given below:

TABLE I

Barium Sulphate Density = 4·432 gm./cm.³

Unit : 10^{11} dynes/cm.²

Plate No.	Description of the plate	Thickness in mm.	Fundamental frequency in Mc/Sec.	Mode of vibration	Effective elastic constant	Value
1	X_1-cut	1·571	1·404	l*	C_{11}	8·622
	do	do	0·786	t*	C_{66}	2·703
	do	do	0·812	t	C_{55}	2·885
2	X_2-cut	1·521	1·495	l	C_{22}	9·166
	do	do	0·822	t	C_{66}	2·771
	do	do	0·550	t	C_{44}	1·241
3	X_3-cut	1·509	1·639	l	C_{33}	10·84
	do	do	0·842	t	C_{55}	2·861
	do	do	0·535	t	C_{44}	1·155
4	X_1 45 X_2	1·689	1·259	l	x_1	8·017
5	X_2 45 X_3	1·872	1·236	l	x_1	9·488
6	X_3 45 X_1	1·917	1·227	l	x_1	9·804

* Here and in the subsequent table, l and t denote the longitudinal and transverse modes respectively.

TABLE II

Strontium Sulphate Density = 3·955 gm./cm.³

Unit : 10^{11} dynes/cm.²

Plate No.	Description of the plate	Thickness in mm.	Fundamental Frequency in Mc/Sec.	Mode of vibration	Effective elastic constant	Value
1	X_1-cut	1·766	1·455	l	C_{11}	10·44
	do	do	0·758	t	C_{55}	2·834
	do	do	0·724	t	C_{66}	2·585
2	X_2-cut	2·061	1·257	l	C_{22}	10·61
	do	do	0·637	t	C_{66}	2·726
	do	do	0·446	t	C_{44}	1·337
3	X_3-cut	1·766	1·615	l	C_{33}	12·86
	do	do	0·746	t	C_{55}	2·745
	do	do	0·525	t	C_{44}	1·360
4	X_1 45 X_2	2·112	1·212	l	x_1	10·36
5	X_2 45 X_3	2·194	1·239	l	x_1	11·68
6	X_3 45 X_1	2·625	1·040	l	x_1	11·79

The values of the elastic constants calculated from the above data are given in Table III.

TABLE III

Unit: 10^{11} dynes/cm.^{2}

Substance	C_{11}	C_{22}	C_{33}	C_{44}	C_{55}	C_{66}	C_{12}	C_{23}	C_{13}
Barytes ..	8·62	9·17	10·84	1·20	2·87	2·74	5·23	3·56	3·41
Celestite ..	10·44	10·61	12·86	1·35	2·79	2·66	7·73	6·19	6·05

The elastic coefficients S's are calculated using the conversion formulæ and are given in Table IV in units of 10^{-13} cm.^{2}/dyne.

TABLE IV

Substance	S_{11}	S_{22}	S_{33}	S_{44}	S_{55}	S_{66}	S_{12}	S_{23}	S_{13}
Barytes ..	18·40	17·36	10·96	83·33	34·84	36·50	− 9·45	−2·73	−2·68
Celestite ..	21·97	21·85	11·42	74·08	35·84	37·59	−13·87	−4·00	−3·66

The linear compressibilities β_1, β_2, β_3 along the principal directions X_1, X_2, X_3 and the volume compressibility β in the above units are calculated using the relations

$$\beta_i = \beta_{i1} + \beta_{i2} + \beta_{i3}, \text{ where } i = 1, 2 \text{ or } 3 \text{ and } \beta = \Sigma \beta_i.$$

TABLE V

Unit: 10^{-13} cm.^{2}/dyne

Substance	β_1	β_2	β_3	β
Barytes ..	6·27	5·18	5·55	17·00
Celestite ..	4·44	3·98	3·76	12·18

5. Discussion of Results

A comparison of the figures given in Tables III and IV shows that the values of elastic constants and elastic coefficients for celestite are higher than those for barytes.

As has been mentioned already, the elastic constants of barytes have been determined by Voigt and Bergmann. Their values along with the author's are given in Table VI.

TABLE VI

Unit: 10^{11} dynes/cm.^{2}

Observer	C_{11}	C_{22}	C_{33}	C_{44}	C_{55}	C_{66}	C_{12}	C_{23}	C_{13}
Voigt ..	8·83	7·85	10·50	1·18	2·85	2·75	4·51	2·65	2·65
Bergmann ..	8·83	7·81	10·38	1·17	2·80	2·55	4·77	2·89	2·69
Author ..	8·62	9·17	10·84	1·20	2·87	2·74	5·23	3·56	3·41

An inspection of the above table shows that the author's values are in general agreement with those of the previous workers but for C_{22} and the cross constants which are slightly higher.

Table VII gives the values of the elastic coefficients S's in units of 10^{-13} cm.^{2}/dyne calculated from the author's C's along with those of the other workers for comparison. The values of S's of Voigt and Bergmann are the same as those quoted by Hearmon (1946).

TABLE VII

Unit: 10^{-13} cm.^{2}/dyne.

Observer	S_{11}	S_{22}	S_{33}	S_{44}	S_{55}	S_{66}	S_{12}	S_{13}	S_{23}
Voigt ..	16·4	18·9	10·6	84·0	34·8	36·0	−9·0	−1·9	−2·5
Bergmann	17·2	19·9	10·9	85·5	35·8	39·2	−9·9	−1·7	−3·0
Author ..	18·40	17·36	10·96	83·33	34·84	36·50	−9·45	−2·68	−2·73

The values of the compressibilities which have been computed from the above values of S's along with the value of β obtained experimentally by Bridgman (1931) are given in Table VIII.

TABLE VIII

Observer	β_1	β_2	β_3	$\beta = \Sigma\beta i$
Voigt ..	5·5	7·4	6·2	19·1
Bergmann ..	5·6	7·0	6·2	18·8
Author ..	6·27	5·18	5·55	17·00
Bridgman ..	..	..	..	17·63

It may be pointed out here that the author's value is nearer the experimental value of Bridgman.

The elastic constants of celestite have been determined for the first time. The value of compressibility for celestite determined by Bridgman (1928) at 30° C. is available in the literature. The values of the principal compressibilities as computed from the author's values of S's lead to a volume compressibility of $12{\cdot}18 \times 10^{-13}$ cm.^{2}/dyne as against Bridgman's value of $16{\cdot}21 \times 10^{-13}$. This discrepancy cannot be accounted for.

Table V shows that barium sulphate is more compressible than strontium sulphate. This may be due to the presence of the heavier barium ion in barytes. This is supported by the fact that the unit cell of barium sulphate is slightly larger than that of strontium sulphate. The dimensions of the edges of the unit cell are:

Barium sulphate	$a_0 = 8{\cdot}89$ A; $b_0 = 5{\cdot}44$ A; $c_0 = 7{\cdot}17$ A
Strontium sulphate	$a_0 = 8{\cdot}36$ A; $b_0 = 5{\cdot}36$ A; $c_0 = 6{\cdot}84$ A

The author takes this opportunity to offer his grateful thanks to Prof. S. Bhagavantam for his guidance and for the interest he has taken in the progress of the present work.

6. Summary

The elastic constants of barium sulphate and strontium sulphate are determined using the wedge method. The values for barytes obtained by Bergmann and Voigt are verified. The elastic constants for strontium sulphate are determined for the first time and they are:

$C_{11} = 10{\cdot}44$; $C_{22} = 10{\cdot}61$; $C_{33} = 12{\cdot}86$; $C_{44} = 1{\cdot}35$; $C_{55} = 2{\cdot}79$; $C_{66} = 2{\cdot}66$; $C_{23} = 6{\cdot}19$; $C_{13} = 6{\cdot}05$; and $C_{12} = 7{\cdot}73$.

References

Bergmann, L. .. *Ultrasonics*, 1938, 179.

Bhagavantam, S. and Bhimasenachar, J. *Proc. Ind. Acad. Sci.*, 1944, **20**, 298.

Bridgman, P. W. *Landolt Börnstein Physikalisch-Chemische Tabellen*, 1931, **II**, Erg., Bd. 1, 33.

——————— .. *International Critical Tables*, 1928, **3**, 50.

Dana, E. S. .. *A Text-book of Mineralogy*, 1947, 748.

Hearmon, R. F. S. .. *Reviews of Modern Physics*, 1946, **18**, 409.

Sundara Rao, R. V. G. .. *Proc. Ind. Acad. Sci.*, 1950, **31A**, 365.

Voigt, W. .. See *Ultrasonics*, by Bergmann, 1938, 179.

SYNTHETIC EXPERIMENTS IN THE BENZOPYRONE SERIES

Part XVI. Isoformononetin and Its Derivatives

By K. Aghoramurthy, N. Narasimhachari and T. R. Seshadri, F.A.Sc.
(From the Department of Chemistry, Delhi University, Delhi)

Received March 21, 1951

In two previous parts of this series[1] earlier experiments on the scope of partial methylation and demethylation for the preparation of 7-methyl ethers of isoflavones were reported with reference to the synthesis of prunetin and santal. The results were quite encouraging and both these naturally occurring 7-methyl ethers were prepared. In support of the theoretical considerations involved, it was felt that simpler cases should be studied in detail and the scope of the method fully understood. Hence the experiments described in this paper were undertaken.

Of the two monomethyl ethers of daidzein (I), formononetin, the 4′-methyl ether (II) was first found to occur in nature.[2] This was first synthesised in poor yield by Wessely *et al.*[3] by heating 2:4-dihydroxy-4′-methoxy-phenyl-benzyl ketone with sodium and ethyl formate in a sealed tube at 100°. Subsequently Mahal, *et al.*[4] employed 2-hydroxy-4-benzyloxy-4′-methoxy-phenyl-benzyl ketone instead of the dihydroxy compound and carried out the reaction at 0° and finally effected the removal of benzyl group. The protection of the 4-hydroxyl group in the ketone is not necessary and a good yield of formononetin has now been obtained directly from the dihydroxy ketone using the low temperature (0°) for the reaction.

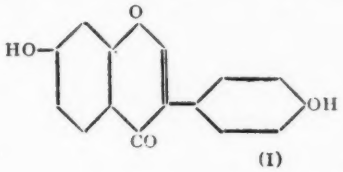

(I)

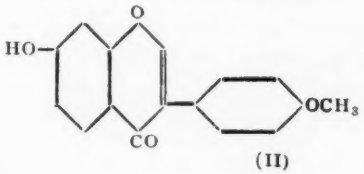

(II)

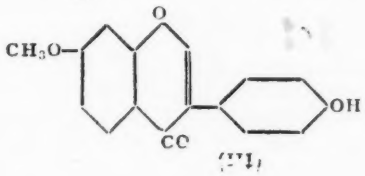

(III)

The isomeric 7-monomethyl ether of daidzein which is now named isoformononetin (III) has not so far been made or described. For its preparation we have employed the partial methylation of daidzein using one mole of dimethyl sulphate. The product is a mixture which could be separated into the following fractions: (1) carbonate soluble; (2) carbonate insoluble but sodium hydroxide soluble; (3) sodium hydroxide insoluble. Fraction (1) obtained by acidifying the carbonate solution consisted of pure daidzein and no formononetin seemed to be present in it. Fraction (2) precipitated from sodium hydroxide solution by acid yielded isoformononetin and fraction (3) which was rather small yielded dimethyl daidzein. The results are in accordance with the theoretical considerations discussed in Part XIII.[1]

The method of partial demethylation was next investigated using O-dimethyl daidzein and hydrobromic acid and hydriodic acid; under suitable conditions almost quantitative yields of isoformononetin could be obtained with these reagents. Heating with hydriodic acid at 120° for half an hour seems to offer the most satisfactory method of partial demethylation for obtaining the 7-methyl ethers of isoflavones.

5:7-Dihydroxy and dimethoxy isoflavones offer the simplest examples for the study of partial methylation and demethylation. Based on analogy with similar flavones and flavanones the existence of large difference between the two hydroxyl groups could be readily understood as also the possibility of partial methylation of the 7-hydroxyl group. For obtaining the 7-methyl ether by demethylation, mild demethylating agents would normally be suggested just as in the case of chrysin dimethyl ether. But in view of our experience with other isoflavones we have now carried out this partial demethylation using hydriodic acid and the method works quite satisfactorily.

5:7-Dihydroxy isoflavone and its methyl ethers were not described till the present work had been completed and the recent paper of Iyer *et al.*[5] containing this description appeared only in March this year. Since our methods and results are slightly different, they are reported in this paper.

2-Hydroxy-4:6-dimethoxy-phenyl-benzyl ketone is conveniently made from phloroglucinol trimethyl ether and phenyl acetyl chloride by condensation in presence of anhydrous aluminium chloride. The product agrees in all its properties with that described by Badcock, *et al.*[6] and Iyer, *et al.*[5] who have made it by a different route. The subsequent isoflavone condensation proceeds quite smoothly giving rise to high yields of 5:7-dimethoxy isoflavone. Partial demethylation of this dimethyl ether with hydriodic acid

gives a very high yield of the 7-monomethyl ether. The interesting point that should be mentioned here is that in the analogous case of chrysin-dimethyl ether using similar conditions the product is found to be mostly chrysin. This reveals the existence of marked difference in the stability of the 7-methyl ether groups in flavones and isoflavones. The explanation is to be found in the difference in the location of the side phenyl nucleus in the two groups of compounds. In flavones the demands of the pyrone C=O group for electrons are met by both the phenyl nuclei whereas in isoflavones the side phenyl plays no part. Consequently in the latter, the 7-position receives a higher quantum of positive charge making this particular hydroxyl more strongly acidic and the methoxyl more firmly held.

Experimental

Formononetin.—Powdered sodium (1 g.) was cooled in ice and treated with a solution of 2:4-dihydroxy-4′-methoxy-phenyl-benzyl ketone (2 g.) in ethyl formate (10 c.c.) with shaking. After keeping in the refrigerator for 48 hours pieces of ice were added and the excess of ethyl formate was removed under reduced pressure. On acidifying the cooled solution formononetin separated as colourless solid and crystallised from alcohol as colourless prisms melting at 255–57°.[3] It dissolved readily in aqueous sodium carbonate solution and gave no colour with ferric chloride in alcoholic solution.

Daidzein.—This was obtained by demethylating formononetin with hydriodic acid (d. 1·7) at 140° for one hour. It crystallised from alcohol as colourless prisms melting at 320–22°. The diacetate crystallised from ethyl acetate as clusters of needles melting at 184–6°.[4]

Partial methylation (*7-Methoxy-4′-hydroxy isoflavone, isoformononetin*).—To a solution of daidzein (0·9 g.) in acetone (100 c.c.) dimethyl sulphate (0·35 c.c.) and potassium carbonate (1 g.) were added and the mixture refluxed for three hours. Acetone was then distilled off and the residue treated with water. The solid that separated was filtered and macerated with sodium carbonate. The residue was then treated with sodium hydroxide solution and the insoluble dimethyl ether was separated by filtration. The dimethyl ether (50 mg.) crystallised from alcohol as colourless needles melting at 154–56°. The alkali solution on acidification gave a colourless solid which crystallised from alcohol as long stout elongated rectangular prisms melting at 218–20°. It was insoluble in cold sodium carbonate solution and gave no colour with ferric chloride in alcoholic solution. Yield, 0·4 g. (Found: C, 71·2; H, 4·5; $C_{16}H_{12}O_4$ requires C, 71·6; H, 4·5%.)

The carbonate solution on acidification gave a colourless solid melting above 310° and one crystallisation from alcohol gave pure daidzein, m.p. 320–22°.

Acetate.—7-Methoxy-4′-hydroxy isoflavone obtained above was acetylated by refluxing with acetic anhydride and pyridine for one hour. The acetate crystallised from ethyl acetate as colourless plates and prismatic needles melting at 148–49° (Found: C, 69·4; H, 4·4; $C_{18}H_{14}O_5$ requires C, 69·7; and H, 4·5%.)

On deacetylation with alcoholic hydrochloric acid and crystallisation from alcohol the isoflavone melted at 218–20°.

7: 4′-*Dimethoxy isoflavone.*—2: 4-Dihydroxy-4′-methoxy-phenyl-benzyl ketone required for this purpose was prepared following the method of Baker and Eastwood,[7] using resorcinol and *p*-methoxy-benzyl cyanide. This was methylated to 2-hydroxy-4: 4′-dimethoxy-phenyl-benzyl ketone using dimethyl sulphate (1 mole) and anhydrous potassium carbonate in acetone solution. It (1 g.) was dissolved in ethyl formate (6 c.c.) and the solution added to pulverised sodium (0·5 g.), cooled in ice and the mixture left in the refrigerator for 48 hours. Crushed ice was then added and ethyl formate removed under reduced pressure. On leaving overnight a colourless solid separated out. It was filtered and the filtrate acidified when some more of the product was obtained. 7: 4′-Dimethoxy isoflavone crystallised from alcohol as colourless needles melting at 154–56°, was insoluble in aqueous sodium hydroxide and gave no colour with ferric chloride.

Partial demethylation

(i) *With hydrobromic acid.*—7: 4′-Dimethoxy isoflavone (0·3 g.) was dissolved in glacial acetic acid (5 c.c.) and heated with hydrobromic acid (d. 1·51; 10 c.c.) for 2 hours on a boiling water-bath. The mixture was then diluted with ice-water and the solid that separated was filtered and washed with water. It was then dissolved in 5% aqueous sodium hydroxide, the solution filtered and the cold alkaline solution acidified with hydrochloric acid. On crystallising from alcohol the product was obtained as colourless long rectangular prisms melting at 218–20°. It was identical with 7-methoxy-4′-hydroxy isoflavone in its properties and a mixed melting point with the sample described above was undepressed.

(ii) *With hydriodic acid.*—7: 4′-Dimethoxy isoflavone (0·4 g.) was dissolved in acetic anhydride (4 c.c.) and treated with cooling with hydriodic acid (10 c.c.; d. 1·7). The solution was heated in an oil-bath at 120° for half an hour. It was then diluted with water, iodine decolourised with

sulphurous acid and left in the refrigerator overnight. The solid that separated was filtered, washed with water and macerated with sodium carbonate solution. The residue was then dissolved in aqueous sodium hydroxide and the clear solution acidified. The product crystallised from alcohol as colourless stout rectangular prisms melting at 218° and was identical with 7-methoxy-4′-hydroxy isoflavone; the mixed melting point with the above two samples was undepressed. Yield, 0·25 g. The acetate crystallised from ethyl acetate as colourless needles and melted at 148–49° alone or in admixture with the other samples already described. The sodium carbonate extract on acidification gave a very small quantity of daidzein.

7-*Methoxy*-4′-*ethoxy isoflavone*.—7-Methoxy-4′-hydroxy isoflavone (0·1 g.) was refluxed in acetone solution with excess of ethyl iodide and anhydrous potassium carbonate for 6 hours. The ethyl ether crystallised from dilute alcohol as colourless short stout prisms melting at 121–22°. It was insoluble in aqueous alkali and gave no colour with ferric chloride in alcoholic solution (Found: C, 73·4; H, 5·2; $C_{18}H_{16}O_4$ requires C, 73·0; H, 5·4%.)

Ethylation of formononetin (*7-ethoxy-4′-methoxy isoflavone*)

Formononetin (0·1 g.) was ethylated as described above. Ethyl formononetin crystallised from alcohol as colourless stout rectangular prisms melting at 141–42° (Found: C, 72·8; H, 5·6; $C_{18}H_{16}O_4$ requires C, 73·0; H, 5·4%.)

2-*Hydroxy*-4 : 6-*dimethoxy-phenyl-benzyl ketone*.—Phloroglucinol trimethyl ether required for this purpose was conveniently obtained by the dry methylation of phloroglucinol with dimethyl sulphate (3 moles) and anhydrous potassium carbonate in acetone solution.

To a solution of anhydrous aluminium chloride (12 g.) and phloroglucinol trimethyl ether (5 g.) in dry ether (100 c.c.) cooled in ice, phenyl acetyl chloride (4 c.c.) was added drop by drop with shaking. The mixture was allowed to stand in the ice-bath for half an hour and then at room temperature for 24 hours. Ether was distilled off and the residue treated with ice and concentrated hydrochloric acid. After warming on a water-bath for 15 minutes the mixture was cooled. The oily liquid soon solidified. It was filtered and washed with dilute hydrochloric acid. The residue was dissolved in aqueous sodium hydroxide and when the solution was acidified it gave a colourless solid. On crystallisation from alcohol it separated as colourless prisms and melted at 117–18°.[5,6] It gave a reddish brown colour with ferric chloride and a blue colour with concentrated nitric acid.

5: 7-*Dimethoxy isoflavone*.—The above ketone (1 g.) was dissolved in ethyl formate (5 c.c.) and cooled in ice. Powdered sodium (0·5 g.) cooled in ice, was then added in small quantities and the mixture left in the refrigerator for 48 hours. Crushed ice was added and excess ethyl formate removed under reduced pressure. On cooling, the oily liquid soon solidified. It crystallised from alcohol as small prisms and melted at 121–2°. Some more of it could be obtained by acidifying the aqueous solution. Yield 0·6 g. Iyer, *et al.*[5] gave its melting point as 120°.

5: 7-*Dihydroxy isoflavone*.—This was obtained by demethylating the dimethoxy compound with hydriodic acid for 3 hours at 140° in an oil-bath. 5 : 7-Dihydroxy isoflavone crystallised from alcohol as colourless prisms melting at 192–4°. It readily dissolved in aqueous sodium carbonate and gave a pink colour with ferric chloride. Its properties agreed with the description of Iyer, *et al.*[5]

5-*Hydroxy*-7-*methoxy isoflavone*

(1) *Partial methylation*.—On methylating with one mole of dimethyl sulphate and anhydrous potassium carbonate in acetone solution for 3 hours 5: 7-dihydroxy isoflavone gave the 7-methyl ether. It crystallised from ethyl acetate as colourless rectangular prisms melting at 140–41°. It gave a red colour with ferric chloride and was sparingly soluble in aqueous sodium hydroxide.

(2) *Partial demethylation*.—5: 7-Dimethoxy isoflavone (0·4 g.) was heated with acetic anhydride (5 c.c.) and hydriodic acid (10 c.c.) at 120° for half an hour and the product worked up as usual. It was macerated with sodium carbonate solution and the residue crystallised. It separated from ethyl acetate in the form of colourless stout rectangular prisms and melted at 141°. (Found: C, 71·2; H, 4·3; $C_{16}H_{12}O_4$ requires C, 71·6; H, 4·5%.) It agreed in all its properties with the sample obtained by method (1) and a mixed melting point was undepressed. The carbonate washings when acidified did not yield any 5: 7-dihydroxy isoflavone.

The above samples agreed with the description of Iyer *et al.*[5]

Summary

The study of daidzein derivatives provides further support to the conclusions already arrived at regarding the special features of partial methylation and demethylation in the isoflavone series. Partial methylation of daidzein gives a good yield of the 7-monomethyl ether (isoformononetin) and the formation of the isomeric formononetin could not be detected. The

same 7-methyl ether is obtained most conveniently by the demethylation of daidzein dimethyl ether with hydrobromic acid and hydriodic acid. 5:7-Dihydroxy and di-methoxy isoflavones have also been examined with a view to compare them with corresponding flavones. 7-Methoxy-5-hydroxy isoflavone is obtained most readily by partial demethylation of dimethoxy isoflavone with hydriodic acid whereas chrysin dimethyl ether yields mostly chrysin under these conditions.

References

1. Narasimhachari and Seshadri .. *Proc. Ind. Acad. Sci.*, 1950, **32 A**, 256 and 342.
2. Lechner and Wessely .. *Br. Chem. Abs.*, 1931, **A**, 738.
3. Kornfeld, Lechner and Wessely .. *Ber.*, 1933, **66 B**, 685.
4. Mahal, Rai and Venkataraman .. *J. C. S.*, 1934, 1769.
5. Iyer, Shah and Venkataraman .. *Proc. Ind. Acad. Sci.*, 1951, **33** A, 116.
6. Badcock, *et al.* .. *J. C. S.*, 1950, 2961.
7. Baker and Eastwood .. *Ibid.*, 1929, 2902.

THE GRAVITATIONAL FIELD OF A RADIATING STAR

By P. C. Vaidya

Senior Research Scholar, Bombay University; V. P. Mahavidyalaya, Vallabh Vidyanagar, Anand)

Received April 27, 1950

(Communicated* by Prof. V. V. Narlikar, F.A.Sc.)

1. Introduction

No non-static solutions, with physical significance, of Einstein's field equations are known outside the field of Cosmology. The field of a radiating mass presents a problem for which general relativity has, so far, not been able to provide a solution. Schwarzschild's external solution deals with the gravitational field of a cold dark body whose mass is constant. The application of this solution to describe the sun's gravitational field should only be regarded as approximate. Various attempts have been made to generalize Schwarzschild's solution in order to make it applicable to non-static masses, (Narlikar, 1936; Narlikar and Moghe, 1936).

While discussing this outstanding unsolved problem of general relativity, Professor Narlikar (1939) remarks:

> "If the principle of energy is to hold good, that is, if the combined energy of the matter and field is to be conserved, the system must be an isolated system surrounded by flat space-time. A spherical radiating mass would probably be surrounded by a finite and non-static envelope of radiation with radial symmetry. This would be surrounded by a radial field of gravitational energy becoming weaker and weaker as it runs away from the central body until at last the field is flat at infinity. It has yet to be seen whether and how this view of the distribution of energy is substantiated by the field equations of relativity."

We represent below the solution of the field equations which substantiates the views expressed above. We begin with the derivation of the energy tensor for the radiation envelope surrounding a star.

---

* The treatment as given here is essentially different from that of Professor H. Mineur as it appears in *Ann. de l'Ecole Normale Superieure*, Ser. 3, **5**, 1, 1933. Our attention was kindly drawn to it by Professor Mineur some years ago. — *V. V. N.* 23-4-1950.

2. Energy Tensor for a Directed Flow of Radiation

By the term "directed flow of radiation" we mean a distribution of electro-magnetic energy such that a local observer at any point of the region of space under consideration finds one and only one direction in which the radiant energy is flowing at the point. Using natural co-ordinates at the point of interest, we may take the components of the energy tensor as being given in terms of electric and magnetic field strengths E and H by the typical examples given by Tolman (1934).

$$T_0^{11} = -\tfrac{1}{2}(E_x^2 - E_y^2 - E_z^2 + H_x^2 - H_y^2 - H_z^2), \tag{2·1}$$

$$T_0^{12} = -(E_x E_y + H_x H_y), \tag{2·2}$$

$$T_0^{14} = (E_y H_z - E_z H_y), \tag{2·3}$$

$$T_0^{44} = \tfrac{1}{2}(E_x^2 + E_y^2 + E_z^2 + H_x^2 + H_y^2 + H_z^2). \tag{2·4}$$

The suffix 0 to a component of a tensor indicates that the component is evaluated in natural co-ordinates at the point of interest. Considering, for simplicity, that the axes of our natural co-ordinates are oriented in such a way that the flow of radiation at the point of interest is in the x-direction and further that the radiation is polarised with the electric vector parallel to y-direction, we shall find

$$E_x = E_z = H_x = H_y = 0; \quad E_y = H_z \tag{2·5}$$

and so the only surviving components of the tensor $T_0^{\mu\nu}$ would be

$$T_0^{11} = T_0^{44} = T_0^{14} = \tfrac{1}{2}(E_y^2 + H_z^2) = \rho, \tag{2·6}$$

ρ being the density of the radiant energy at the point.

Having obtained the components of $T^{\mu\nu}$ for one system of co-ordinates, we can find them in any other system by the rules of tensor transformation. For a general co-ordinate system with the line-element

$$ds^2 = g_{\mu\nu} dx^\mu dx^\nu, \tag{2·7}$$

the components of $T^{\mu\nu}$ will be given by

$$T^{\mu\nu} = \frac{\partial x^\mu}{\partial x^\alpha}_0 \frac{\partial x^\nu}{\partial x^\beta}_0 T_0^{\alpha\beta}. \tag{2·8}$$

On using (2·6) this yields

$$T^{\mu\nu} = \left[\frac{\partial x^\mu}{\partial x_0^1}\frac{\partial x^\nu}{\partial x_0^1} + \frac{\partial x^\mu}{\partial x_0^4}\frac{\partial x^\nu}{\partial x_0^4} + \frac{\partial x^\mu}{\partial x_0^1}\frac{\partial x^\nu}{\partial x_0^4} + \frac{\partial x^\mu}{\partial x_0^4}\frac{\partial x^\nu}{\partial x_0^1}\right]\rho. \tag{2·9}$$

As the radiant energy travels along null-geodesics

$$dx_0^1 = dx_0^4 = d\tau \text{ (say)}. \tag{2·10}$$

By (2·10) along the radiation flow we find

$$g_{\mu\nu}dx^{\mu}dx^{\nu}=0. \tag{2·11}$$

Next we use (2·10) in

$$\frac{dx^{\mu}}{d\tau}=\frac{\partial x^{\mu}}{\partial x_0{}^{a}}\frac{dx_0{}^{a}}{d\tau}$$

and find

$$\frac{dx^{\mu}}{d\tau}=\frac{\partial x^{\mu}}{\partial x_0{}^{1}}+\frac{\partial x^{\mu}}{\partial x_0{}^{4}}\,. \tag{2·12}$$

With the help of (2·12), (2·9) finally reduces to

$$T^{\mu\nu}=\rho\frac{dx^{\mu}}{d\tau}\frac{dx^{\nu}}{d\tau}\,, \tag{2·13}$$

with

$$g_{\mu\nu}\frac{dx^{\mu}}{d\tau}\frac{dx^{\nu}}{d\tau}=0. \tag{2·14}$$

Thus for our case of the outside field of a non-static mass the energy tensor is to be taken of the form

$$T^{\mu\nu}=\rho v^{\mu}v^{\nu}, \tag{2·15}$$

with

$$v_{\mu}v^{\mu}=0;\ \ (v^{\mu})_{\nu}\,v^{\nu}=0. \tag{2·16}$$

3. The Field Equations

A star of mass M and radius r_0 is supposed to start radiating at time t_0. As the star continues to radiate the zone of radiation increases in thickness, its outer surface at a later instant t_1 being $r=r_1$. For $r_0\leqslant r\leqslant r_1$, $t_0\leqslant t\leqslant t_1$ let the line-element be assumed to be of the form

$$ds^2=-e^{\lambda}dr^2-r^2(d\theta^2+\sin^2\theta d\phi^2)+e^{\nu}dt^2,$$
$$\lambda=\lambda(r,t),\ \ \nu=\nu(r,t). \tag{3·1}$$

For the nature of radiation we have found the energy tensor $T^{\mu\nu}$ of the form

$$T^{\mu\nu}=\rho v^{\mu}v^{\nu}, \tag{3·2}$$

ρ is the density of radiation and the lines of flow are null-geodesics:

$$v_{\mu}v^{\mu}=0;\ \ (v^{\mu})_{\nu}\,v^{\nu}=0. \tag{3·3}$$

Since $(T^{\mu\nu})_{\nu}=0$, we have the analogue of the equation of continuity

$$(\rho v^{\mu})_{\mu}=0. \tag{3·4}$$

As the flow is to be radial, $v^2=0$, $v^3=0$ and

$$T_1{}^1=\rho v_1v^1,\ T_4{}^4=\rho v_4v^4,\ T_1{}^4=\rho v_1v^4,\ T_2{}^2=T_3{}^3=0. \tag{3·5}$$

Also $v_\mu v^\mu = 0$ simplifies to

$$-e^{\lambda}(v^1)^2 + e^{\nu}(v^4)^2 = 0. \tag{3·6}$$

With the usual expression for the components of $T^{\mu\nu}$ in terms of $g_{\mu\nu}$ and their derivatives, (3·5) gives the following three field equations:

(i) $$T_1^4 e^{(\nu-\lambda)/2} + T_4^4 = 0, \tag{3·7}$$

or $$e^{-\lambda}\left(\frac{\lambda'}{r} - \frac{1}{r^2}\right) + \frac{1}{r^2} + \frac{\dot{\lambda}}{r} e^{-(\lambda+\nu)/2} = 0; \tag{3·8}$$

(ii) $$T_1^1 + T_4^4 = 0, \tag{3·9}$$

or $$e^{-\lambda}\left(\frac{\lambda' - \nu'}{r} - \frac{2}{r^2}\right) + \frac{2}{r^2} = 0; \tag{3·10}$$

(iii) $$T_2^2 = 0, \tag{3·11}$$

or $$-e^{-\lambda}\left(\frac{\nu''}{2} + \frac{\nu'^2}{4} - \frac{\lambda'\nu'}{4} + \frac{\nu' - \lambda'}{2r}\right) + e^{-\nu}\left(\ddot{\lambda} + \frac{\dot{\lambda}^2}{4} - \frac{\dot{\lambda}\dot{\nu}}{4}\right) = 0. \tag{3·12}$$

Here and in what follows an overhead dash or dot indicates a differentiation with regard to r or t.

If the total energy is to be conserved, the line-element obtained by solving these equations must reduce to the static form

$$ds^2 = -\left(1 - \frac{2M}{r}\right)^{-1} dr^2 - r^2(d\theta^2 + \sin^2\theta d\phi^2) + \left(1 - \frac{2M}{r}\right) dt^2 \tag{3·13}$$

at $r = r_0$, $t = t_0$ and for $r \geqslant r_1$ at $t = t_1$.

4. The Solution of the Field Equations

On putting $$e^{-\lambda} = 1 - \frac{2m}{r}, \quad m = m(r, t) \tag{4·1}$$

in the field equation (3·8) we find that it is equivalent to

$$e^{-\lambda/2}\frac{\partial m}{\partial r} + e^{-\nu/2}\frac{\partial m}{\partial t} = 0. \tag{4·2}$$

Using the operator

$$\frac{d}{d\tau} \equiv v^1\frac{\partial}{\partial r} + v^4\frac{\partial}{\partial t}, \tag{4·3}$$

we may express this as

$$\frac{dm}{d\tau} = 0. \tag{4·4}$$

From (4·2) we can express $e^{\nu/2}$ in terms of m:

$$e^{\nu/2} = -\frac{\dot{m}}{m'}\left(1-\frac{2m}{r}\right)^{-1/2}. \tag{4·5}$$

Now we can take the second field equation (3·10). On substituting the values of λ and ν from (4·1) and (4·5), we find that

$$\left(\frac{\dot{m}'}{\dot{m}} - \frac{m''}{m'}\right)\left(1-\frac{2m}{r}\right) = \frac{2m}{r^2}. \tag{4·6}$$

The first integral of the above equation is

$$m'\left(1-\frac{2m}{r}\right) = f(m), \tag{4·7}$$

$f(m)$ being an arbitrary function. (4·7) is the differential equation to be solved for m.

We now take the third field equation (3·12). We shall show that when λ and ν are given by (4·1), (4·5) together with the last differential equation (4·7), the equation (3·12) is automatically satisfied. The following is an identity holding between the components of the tensor $T_\mu{}^\nu$.

$$\frac{\partial}{\partial r}(T_1{}^1) + \frac{\partial}{\partial t}(T_1{}^4) - \frac{\nu'}{2}(T_4{}^4 - T_1{}^1) + \frac{2}{r}(T_1{}^1 - T_2{}^2) + T_4{}^4\left(\frac{\dot{\lambda}}{2} + \dot{\nu}\right) = 0. \tag{4·8}$$

With the help of this identity and the two equations (3·7) and (3·9) the equation (3·11) can be transformed into

$$\frac{d}{d\tau}(r^2 e^{-\lambda} T_4{}^4) = 0. \tag{4·9}$$

Thus the third field equation is satisfied, *i.e.*, $T_2{}^2 = 0$ provided (4·9) is satisfied, *i.e.*, provided

$$\frac{d}{d\tau}\left\{m'\left(1-\frac{2m}{r}\right)\right\} = 0, \tag{4·10}$$

i.e., provided $\frac{dm}{d\tau} = 0$ when we use (4·7). And the last relation is already proved as (4·4) above.

Hence we have solved all the field equations and the final line-element describing the radiation envelope of a star is

$$ds^2 = -\left(1-\frac{2m^{-1}}{r}\right)dr^2 - r^2(d\theta^2 + \sin^2\theta d\phi^2) + \frac{\dot{m}^2}{f^2}\left(1-\frac{2m}{r}\right)dt^2, \tag{4·11}$$

with $$m'\left(1-\frac{2m}{r}\right)=f(m),\ m=m(r,t)$$

for $$r_0 \leqslant r \leqslant r_1,\ t_0 \leqslant t \leqslant t_1.$$

The surviving components of energy tensor are

$$-T_1{}^1=T_4{}^4=\frac{m'}{4\pi r^2},\ T_1{}^4=\frac{m'^2}{4\pi\dot{m}r^2},\ T_4{}^1=-\frac{\dot{m}}{4\pi r^2}. \tag{4·12}$$

(Vaidya, 1943).

5. The Operator $\frac{d}{d\tau}$

The relation (4·4)

$$\frac{dm}{d\tau}=0 \tag{5·1}$$

is a type of relation peculiar to the field we are investigating. In this section we obtain some more relations of this type. On eliminating v^4 from $v_\mu v^\mu=0$ and $(v^\mu)_\nu\, v^\nu=0$ we find

$$\frac{\partial v^1}{\partial r}+\frac{\partial v^1}{\partial t}e^{(\lambda-\nu)/2}+v^1\left(\frac{\lambda'+\nu'}{2}+\dot{\lambda}\,e^{(\lambda-\nu)/2}\right)=0. \tag{5·2}$$

But the last term on the left hand side can be shown to vanish by using the field equations (3·8) and (3·10). Hence (5·2) becomes

$$\frac{dv^1}{d\tau}=0. \tag{5·3}$$

Another such relation can be obtained by starting with the equation of continuity (3·4)

$$(\rho v^\mu)_\mu=0$$

which when written out in full gives

$$\frac{\partial}{\partial x^\mu}(r^2\sin\theta\rho v^\mu e^{(\lambda+\nu)/2})=0. \tag{5·4}$$

When v^4 is eliminated again we find

$$\frac{\partial}{\partial r}(r^2\rho v^1)+e^{(\lambda-\nu)/2}\frac{\partial}{\partial t}(r^2\rho v^1)+(r^2\rho v^1)\left(\frac{\lambda'+\nu'}{2}+\dot{\lambda}e^{(\lambda-\nu)/2}\right)=0. \tag{5·5}$$

Like (5·2) this also reduces further to give

$$\frac{d}{d\tau}(r^2\rho v^1)=0. \tag{5·6}$$

(5·3) and (5·6) together can be used to obtain

$$\frac{d}{d\tau}(r^2\rho v^1 v^1)=0 \quad \text{or} \quad \frac{d}{d\tau}(r^2T^{11})=0 \tag{5·7}$$

and $$\frac{d}{d\tau}(r^2\rho) = 0 \qquad (5\cdot8)$$

the former of which would again imply $T_2{}^2 = 0$ as seen in the last section.

From the definition of the operator

$$\frac{d}{d\tau} \equiv v^1 \frac{\partial}{\partial r} + v^4 \frac{\partial}{\partial t},$$

it is clear that it differentiates following the lines of flow. Hence the relations (5·1), (5·3) and (5·8) show that m, v^1 and $r^2\rho$ are conserved along the lines of flow. Here we shall try to understand the phrase " conserved along a line of flow ". At any time t, a spherical wave-front of radius $r =$ the radius of the star starts moving onwards. At every point of this wave-front the functions m, v^1, $r^2\rho$ have certain values at the start. The functions will retain these values at any point of this wave-front throughout the motion of the wave-front. The boundary $r = r_1$ at $t = t_1$ is a wave-front. At $t = t_0$, this wave-front started moving with radius $r = r_0$. At that time the value of m on the wave-front was M the total mass of the star. Our conservation result now asserts that on this first wave-front, the value of m will always be M. Thus at $t = t_1$ on the boundary of the radiation zone $r = r_1$ we find $m = \mathrm{M}$.

We may add some simple mathematical properties of the conserved results. If

$$\frac{d\psi}{d\tau} = 0,$$

in our co-ordinate system, it means

$$g^{\mu\nu} \frac{\partial\psi}{\partial x^\mu} \frac{\partial\psi}{\partial x^\nu} = 0$$

which means that $\partial\psi/\partial x^\mu$ is a null-vector.

It follows that

$$\left(\frac{\partial\psi}{\partial x^\alpha} g^{\alpha\epsilon}\right)_\beta \frac{\partial\psi}{\partial x^\sigma} g^{\sigma\beta} = 0. \qquad (5\cdot9)$$

For a line-element of the form (3·1), we have from (5·9) that if

$$\frac{d\psi}{d\tau} = 0, \quad \frac{d}{d\tau}(e^{-\lambda}\psi') = 0 \qquad (5\cdot10)$$

which will show that (4·10) is a consequence of (4·4).

The actual values of v^1 and v^4 may now be deduced. From (5·1) and (5·3) we have

$$\frac{\partial v^1}{\partial r} - \frac{m'}{\dot{m}} \frac{\partial v^1}{\partial t} = 0. \tag{5·11}$$

Hence

$$v^1 = \phi(m), \quad v^4 = -\frac{m'}{\dot{m}} \phi(m). \tag{5·12}$$

$\phi(m)$ is now to be obtained by using any one of the equations

$$-T_1^1 = T_4^4 = \frac{m'}{4\pi r^2}, \quad T_1^4 = \frac{m'^2}{4\pi \dot{m} r^2}, \quad T^4{}_1 = -\frac{\dot{m}}{4\pi r^2}.$$

Thus $4\pi r^2 \rho v_4 v^1 = -\dot{m}$

or

$$\{\phi(m)\}^2 = \frac{m'}{4\pi r^2 \rho}\left(1 - \frac{2m}{r}\right)$$

or

$$v^1 = \left\{\frac{f(m)}{4\pi r^2 \rho}\right\}^{1/2}, \quad v^4 = -\frac{m'}{\dot{m}} \left\{\frac{f(m)}{4\pi r^2 \rho}\right\}^{1/2}. \tag{5·13}$$

6. The Boundary of the Radiation Zone

For the field of the radiation zone of a star we have two boundaries: (1) the boundary separating radiation from the material contents (or the internal) of the star and (2) the outer expanding boundary of the radiation zone separating it from 'empty' space beyond. We shall try to find the conditions at these boundaries which will ensure a unique solution.

The line-element under discussion is

$$ds^2 = -\left(1 - \frac{2m}{r}\right)^{-1} dr^2 - r^2(d\theta^2 + \sin^2\theta d\phi^2) + \frac{\dot{m}^2}{f^2}\left(1 - \frac{2m}{r}\right) dt^2, \tag{6·1}$$

$$m'\left(1 - \frac{2m}{r}\right) = f(m). \tag{6·2}$$

It contains two arbitrary functions. $f(m)$ is one of them. The other is an arbitrary function of t, say $\phi(t)$, which appears when we solve the partial differential equation (6·2) for m.

The expanding bounding surface of the radiation zone has been taken to be a sphere of radius $r = r_1$ at a time $t = t_1$. Obviously r_1 and t_1 are interconnected. We shall now say that this bounding surface is a sphere of variable radius $r = R(t)$ which would, of course, mean that $R(t_1) = r_1$.

Beyond the bounding sphere of the radiation zone the space is 'empty' and the line-element is

$$ds^2 = -\left(1 - \frac{2M}{r}\right)^{-1} dr^2 - r^2 (d\theta^2 + \sin^2\theta d\phi^2) + \left(1 - \frac{2M}{r}\right) dt^2. \quad (6\cdot3)$$

We show now, that the continuity of $g_{\mu\nu}$ at $r = R(t)$ will be sufficient, firstly, to locate the boundary at any time t, *i.e.*, to determine the function $R(t)$, secondly, to find out the arbitrary function $\phi(t)$ and thirdly to ensure that the total energy of the distribution is M.

Let
$$V(m, r) = \phi(t) \quad (6\cdot4)$$

be the general solution of the equation

$$\frac{\partial m}{\partial r}\left(1 - \frac{2m}{r}\right) = f(m)$$

the condition for which is

$$\frac{\partial V}{\partial r}\left(1 - \frac{2m}{r}\right) = -f(m)\ \frac{\partial V}{\partial m}. \quad (6\cdot5)$$

The value of $\dot{m}$ is given by

$$\frac{\partial V}{\partial m}\dot{m} = \dot{\phi}. \quad (6\cdot6)$$

Continuity of $g_{\mu\nu}$ gives, at $r = R(t)$

$$m = M$$
$$\dot{m} = -f(M).$$

(6·4) and (6·6) then give

$$V(M, R) = \phi(t) \quad (6\cdot7)$$

$$-f(M)\frac{\partial V}{\partial M} = \dot{\phi}. \quad (6\cdot8)$$

Here $\frac{\partial V}{\partial M}$ and $\frac{\partial V}{\partial R}$ denote the values of the derivatives $\frac{\partial V}{\partial m}$ and $\frac{\partial V}{\partial r}$ respectively at $m = M$, $r = R$; which is equivalent to saying that they denote the corresponding partial derivatives of V when the variables m and r in V are replaced by M and R. (6·7) and (6·8) are the equations to determine the two functions $R(t)$ and $\phi(t)$.

To eliminate $\phi(t)$ between (6·7) and (6·8) we differentiate (6·7) with respect to t, to get

$$\frac{\partial V}{\partial R}\dot{R} = \dot{\phi}$$

which with (6·8) gives

$$\frac{\partial V}{\partial R}\dot{R} = -f(M)\frac{\partial V}{\partial M}. \tag{6·9}$$

We shall now compare (6·9) with (6·5). (6·5) is a relation in m and r. When $m = M$, $r = R$, it becomes

$$\frac{\partial V}{\partial R}\left(1 - \frac{2M}{R}\right) = -f(M)\frac{\partial V}{\partial M}. \tag{6·10}$$

Comparing (6·9) and (6·10) we find

$$\dot{R} = 1 - \frac{2M}{R}.$$

The general solution of this last differential equation is

$$R + 2M \log (R - 2M) - t = \text{a contsant},$$

which in our former notation, would mean that if the boundary of the radiation zone is $r = r_1$ at a time $t = t_1$,

$$r_1 + 2M \log (r_1 - 2M) - t_1 = \text{a constant}. \tag{6·11}$$

The function $\phi(t)$ is now given by (6·7). It is interesting to note that the boundary radius $r = R(t)$ is determined independently of the nature of the function $V(m, r)$.

Before we proceed further let us study the condition $\dot{m} = -f(M)$ at $r = R(t)$. It says that, at all times, on the boundary of the radiation zone, $\dot{m}$ is a constant. But $\dot{m}$ is not conserved along a line of flow. Using the explanations of the last section, we say that the radiating star goes on emitting a series of wave-fronts. As $\dot{m}$ is not a conserved function, it is not constant for each one of these wave-fronts. But as m contains an arbitrary function of t, it is possible to select this function in such a way that $\dot{m}$ takes up a constant value on a particular wave-front. And this is what we have done by the condition (6·8). Note that the continuity of $g_{\mu\nu}$ at $r = R$ ensures that at the start, $r = r_0$, $t = t_0$, the line-eliment is again (6·3).

The conditions at the boundary $r = R(t)$ have left $f(m)$ undetermined. We expect that $f(m)$ will be determined by the conditions at the inner boundary of the star. It is clear that $f(m)$ is governed by the conditions in the interior of the star, different stellar models giving different forms of $f(m)$. That this will be the case, can be very easily seen from the definition of $f(m)$:

$$f(m) = m'\left(1 - \frac{2m}{r}\right)$$

or approximately $f(m)=m'$ or again $f(m)=-\dot{m}$, because m' is almost equal to $-\dot{m}$. Thus $f(m)$ measures the luminosity of the star, at the Newtonian level of approximation.

Lastly we may now verify that the principle of conservation of energy holds good. The line-element (3·1) can be expressed in the form

$$ds^2=-\{(dx)^2+(dy)^2+(dz)^2\}-\frac{e^{\lambda}-1}{r^2}(xdx+ydy+zdz)^2+e^{\nu}dt^2 \tag{6·12}$$

By using the well-known formulæ[1] the energy content of (6·12) is found to be

$$\mathrm{E}=\lim_{r\to\infty}\{\tfrac{1}{2}r(e^{\lambda}-1)e^{(\nu-\lambda)/2}\}. \tag{6·13}$$

Hence for all distributions for which the line-element (3·1) goes off continuously over some boundary to the Schwarzschild's form (6·3), the principle of conservation

$$\mathrm{E}=\mathrm{M}$$

holds good.

7. The Electro-Magnetic Field

The outside of a radiating star is the seat of electro-magnetic phenomena. So the field which we have considered above must be capable of being obtained from an electro-magnetic potential K_{μ}. That this is the case, has been already shown elsewhere (Narlikar and Vaidya, 1947, 1948).

8. Particular Solutions of the Equation $m'\left(1-\frac{2m}{r}\right)=f(m)$

We shall here solve the equation

$$\frac{\partial m}{\partial r}\left(1-\frac{2m}{r}\right)=f(m) \tag{8·1}$$

under different assumptions for $f(m)$.

Case (1): Let $f(m)$ be a constant.

$$f(m)=k<\tfrac{1}{8}.$$

m is given by the algebraic equation $(m-\alpha r)^{\mathrm{A}}(m-\beta r)^{\mathrm{B}}=\phi(t)$.

Here $$\alpha,\beta=\tfrac{1}{4}\{1\pm(1-8k)^{1/2}\};$$

$$\mathrm{A},\mathrm{B}=\tfrac{1}{2}\{1\mp(1-8k)^{-1/2}\}.$$

$\phi(t)$ is an arbitrary function of t.

[1] Formula (91·1) on p. 232 of Relativity Thermodynamics and Cosmology by R. C. Tolman (1934) was used.

Next let $f(m)=k=\frac{1}{8}$.

m is given by the algebraic equation $r=4(m-r)\{\log(4m-r)+\phi(t)\}$.

Finally let $f(m)=k>\frac{1}{8}$. m is given by the equation

$$2\tan^{-1}\left\{\left(\frac{4m}{r}-1\right)(8k-1)^{-1/2}\right\}=(8k-1)^{\frac{1}{2}}\log(2m^2-mr+kr^2)+\phi(t).$$

Case (2): Some more particular solutions may be obtained by trying the following method. The condition that the total differential equation

$$m'dr+\dot{m}dt-dm=0 \tag{8·2}$$

should be exact is given by

$$\frac{dt}{0}=\frac{dr}{1}=\frac{(r-2m)\,dm}{rf(m)}=\frac{(r-2m)\,d(\dot{m})}{r\dot{m}\left\{\frac{df}{dm}+2f(r-2m)^{-1}\right\}}. \tag{8·3}$$

Solving (8·3) we try to obtain $\dot{m}$ as a function of m, r and t. Then this $\dot{m}$ and m' from (8·1) will make (8·2) exact. The solution of (8·2) will therefore give us the final solution for m. It can now be verified that the following is a solution of (8·3)

$$\dot{m}(r-2m)(m-\alpha r)^n(m-\beta r)^n\gamma=\phi(t) \tag{8·4}$$

where
$$(\alpha+\beta)2n=-1,\quad \alpha^n\beta^n\gamma\cdot f(m)=k^n \tag{8·5}$$

$$\alpha=\alpha(m),\ \beta=\beta(m),\ \gamma=\gamma(m),\ k=\text{a constant}, \tag{8·6}$$

$$\left(\frac{f(m)}{2}+\frac{4n+1}{n^2}\right)=k(3+2n)\left(f(m)\,\gamma\right)^{-n} \tag{8·7}$$

and $f(m)$ is to be taken as

$$\left(\frac{f(m)}{m}+\frac{1}{m}\frac{1+n}{2n^2}\right)^{4(1+n)}=c\left(4f(m)+\frac{1+2n}{2n}\right)^{1+2n}. \tag{8·8}$$

n, c are constants and $1+n\neq 0$, $3+2n\neq 0$. Various cases follow from this solution for different values of n.

Case (3): $1+2n=0$, $f(m)=cm-1$, c a constant. Then

$$m'\left(1-\frac{2m}{r}\right)=cm-1,$$

$$4c\dot{m}^2(r-2m)^2=\dot{\phi}^2(cm-1)^2(cr^2-4r+4n).$$

The complete solution for m is

$$2\left(r^2-\frac{4r}{c}+\frac{4m}{c}\right)^{1/2}+\frac{4}{c}\log\left\{\left(r-\frac{2}{c}\right)+\left(r^2-\frac{4r}{c}+\frac{4m}{c}\right)^{1/2}\right\}$$
$$-\frac{2}{c}\log(cm-1)=\phi(t).$$

Case (4): Let $5 + 6n = 0$ then $50f(m) = (625\,cm + 36)^{1/2}$, c a constant.

$$\frac{\dot{m}(r-2m)}{f(m)} X(m, r) = \dot{\phi}, \left(\frac{3f}{8} + \frac{9}{200}\right)^{5/6} = X. \quad \left(m^2 - \frac{3}{5}mr + \frac{3f}{8} + \frac{9}{200}\right)^{5/6}.$$

The final (m, r) relation is given by

$$V = \int \left(\frac{\partial V}{\partial m} + \frac{r-2m}{f} X\right) dm,$$

where the integrand on the right hand side will be a function of m only and

$$V = \int Xr\,dr + \phi(t).$$

In the last expression while performing the integration with respect to r, m is to be treated as a constant.

My thanks are due to Professor V. V. Narlikar for having suggested this problem and for general guidance during the work.

Summary

A star of mass M and radius r_0 is supposed to start radiating at time t_0. The zone of radiation extends to $r = r_1$ at a later instant $t = t_1$. The energy tensor for the radiation zone, describing the directed flow of radiation, is evaluated and a relativistic line-element representing the field of radiation for $r_0 \leqslant r \leqslant r_1$ and corresponding $t_0 \leqslant t \leqslant t_1$ is obtained. It is shown that certain quantities m, v^1, $r^2\rho$, etc., are conserved in the field along a world-line of flow. At $r = r_0$, $t = t_0$ and at $r = r_1$, $t = t_1$, the line-element reduces to Schwarzschild's static form for a mass M. The conservation of energy is verified. The electro-magnetic potential K_μ of this field has already been obtained elsewhere.

References

1. Narlikar, V. V. .. *Bombay Uuiv. J.*, 1939, **8**, 31.
2. ———— .. *Phil. Mag.*, 1936, **22**, 767.
3. ——— and Moghe, D. N. .. *Proc. Nat. Acad. Sci.*, India, 1936, **6**, 97.
4. ——— and Vaidya, P. C. .. *Nature*, 1947, **159**, 642.
5. ———— .. *Proc. Nat. Inst. Sci.*, India, 1948, **14**, 53.
6. Tolman, R. C. .. *Relativity, Thermodynamics and Cosmology*, 1934, 270.
7. Vaidya, P. C. .. *Curr. Sci.*, 1943, **12**, 183.

NOTE ON A PAIR OF FUNCTIONAL EQUATIONS SATISFIED BY $T_n(z)$

BY HARI DAS BAGCHI AND BHOLA NATH MUKHERJEE

(Communicated by Prof. B. S. Madhava Rao)

Received January 11, 1950

Art. 1.—It is well known that Tschebyscheff's function $T_n(z)$ forms a particular solution of the functional equation:

$$f_{n+1}(z) - zf_n(z) + \tfrac{1}{4} f_{n-1}(z) = 0, \qquad (n > 1) \qquad \text{(I)}$$

as also of the differential equation:

$$(1 - z^2)\frac{d^2w}{dz^2} - z\frac{dw}{dz} + n^2w = 0. \qquad \text{(A)}$$

It is interesting to verify that $T_n(z)$ satisfies another functional equation, *viz.*,

$$(1 - z^2) f_n'(z) + n\{f_{n+1}(z) - \tfrac{1}{4} f_{n-1}(z)\} = 0, \qquad (n \geqslant 1). \qquad \text{(II)}$$

We shall write (I) and (II) in the equivalent forms,

$$\tfrac{1}{2} f_{n-1}(z) = zf_n(z) - \frac{1}{n}(z^2 - 1) f_n'(z) \qquad \text{(III)}$$

and

$$2f_{n+1}(z) = zf_n(z) + \frac{1}{n} \cdot (z^2 - 1) f_n'(z). \qquad \text{(IV)}$$

We now propose to investigate all possible *common* solutions of (I) and (II) or what is the same thing (III) and (IV). We shall henceforth refer to the differential equation (A) as the T-equation of *rank* n and symbolise it as $T^{(n)}$.

To fix our ideas, suppose that for *some fixed value* of n, $f_n(z)$ is an arbitrary solution of the equation $T^{(n)}$, so that

$$(1-z^2) \cdot f_n''(z) - zf_n'(z) + n^2 f_n(z) = 0. \qquad (1)$$

Then introduce the two "*contiguous*" functions $f_{n-1}(z)$ and $f_{n+1}(z)$ in accordance with the relations (III) and (IV).

Differentiating (IV) and utilising (1), we find

$$2f_{n+1}'(z) = (n + 1)\left\{f_n(z) + \frac{z}{n} f_n'(z)\right\}. \qquad (2)$$

A second differentiation, combined with (II), leads to:

$$2f_{n+1}''(z)=\left[\frac{(n+1)^2}{n}+\frac{n+1}{n}\cdot\frac{z^2}{1-z^2}\right]\cdot f_n'(z)-\frac{n(n+1)z}{1-z^2}\cdot f_n(z). \tag{3}$$

The relations (2) and (3) accord with the relation:

$$(1-z^2)f_{n+1}''(z)-zf_{n+1}'(z)+(n+1)^2f_{n+1}(z)=0, \tag{4}$$

showing that $f_{n+1}(z)$ satisfies $\mathrm{T}^{(n+1)}$.

Further, from (IV) and (2) we get:

$$2\left[zf_{n+1}(z)-\frac{1}{n+1}\cdot(z^2-1)f_{n+1}'(z)\right]$$

$$=z\left\{zf_n(z)+\frac{1}{n}(z^2-1)f_n'(z)\right\}-\frac{z^2-1}{n+1}\cdot(n+1)\left\{f_n(z)+\frac{zf_n'(z)}{n}\right\}$$

$$=f_n(z),$$

i.e.,
$$\tfrac{1}{2}f_n(z)=zf_{n+1}(z)-\frac{1}{n+1}\cdot(z^2-1)f_{n+1}'(z). \tag{5}$$

This signifies that $f_n(z)$ is one of the two functions "contiguous" to $f_{n+1}(z)$.

If we now define the second "contiguous" function $f_{n+2}(z)$ of $f_{n+1}(z)$ by:

$$2f_{n+2}(z)=zf_{n+1}(z)+\frac{1}{n+1}\cdot(z^2-1)f_{n+1}'(z), \tag{6}$$

and recognise that the other "contiguous" function of $f_{n+1}(z)$, *viz.*, $f_n(z)$, satisfies a relation, *viz.*, (5), which is *similar* in form to the equation (III) for $f_{n-1}(z)$, we infer on the strength of the results proved before that $f_{n+2}(z)$ satisfies $\mathrm{T}^{(n+2)}$. Proceeding in this way, we derive an "*ascending*" sequence of functions, *viz.*,

$$f_n(z), f_{n+1}(z), f_{n+2}(z), \tag{7}$$

which conform respectively to the sequence of differential equations:

$$\mathrm{T}^{(n)}, \mathrm{T}^{(n+1)}, \mathrm{T}^{(n+2)},$$

and between any two contiguous members of which there subsist the two functional relations (I) and (II).

We shall now look for a "descending" sequence of functions, possessing similar properties.

For this purpose we may differentiate (III) and utilise (I), so as to deduce

$$\tfrac{1}{2}f_{n-1}'(z)=(n-1)\cdot\left\{\frac{z}{n}f_n'(z)-f_n(z)\right\}. \tag{8}$$

Another differentiation combined with (1) leads to:

$$\tfrac{1}{2}f_{n-1}''(z)=\left[-\frac{(n-1)^2}{n}+\frac{n-1}{n}\cdot\frac{z^2}{1-z^2}\right]f_n'(z)-\frac{n(n-1)}{1-z^2}\cdot f_n(z). \quad (9)$$

Manifestly (III), (8) and (9) abide by the relation $T^{(n-1)}$, *viz.*,

$$(1-z^2)\cdot f_{n-1}''(z)-zf_{n-1}'(z)+(n-1)^2 f_{n-1}(z)=0. \quad (10)$$

Repetition of the previous line of argument leads to a "descending" sequence of functions:

$$f_n(z),\ f_{n-1}(z), f_{n-2}(z),\ldots,f_0(z), \quad (11)$$

satisfying the sequence of equations of the type $\{T^{(n)}\}$ and at the same time the pair of functional equations (I), (II) or (III), (IV).

It is scarcely necessary to add that, whereas the "ascending" sequence (7) comprises an *infinite* number of elements, the "descending" sequence (11) comprises only a *finite* number.

Art. 2.—It is now easy to make use of the results of the foregoing article to investigate the *common* solutions of the sequence of differential equations of the type $T^{(n)}$ and of the pair of functional equations (I) and (II). The needful for this is to take the *initially fixed* value of n, as contemplated in § 1, to be *unity*. That is to say, we have to start with an arbitrary solution $f_1(z)$ of $T^{(1)}$, so that

$$(1-z^2)\cdot f_1''(z)-zf_1'(z)+f_1(z)=0. \quad (12)$$

Application of the foregoing process at once places at our disposal a sequence of functions, beginning with $f_1(z)$, *viz.*,

$$f_1(z),\ f_2(z),\ \ldots,\ f_n(z),\ \ldots\ldots,$$

which are compatible with (I) and (II) or (III) and (IV). As regards $f_0(z)$, which is one of the two functions, "contiguous" to $f_1(z)$, we have, on putting $n=1$ in (III),

$$f_0(z)=2\{(1-z^2)\cdot f_1'(z)+zf_1(z)\}. \quad (13)$$

In as much as the left side of (12) is

$$=\frac{d}{dz}\cdot\{(1-z^2)\cdot f_1'(z)+zf_1(z)\},$$

we get

$$(1-z^2)\cdot f_1'(z)+zf_1(z)=\text{const. (say, } c); \quad (14)$$

so that

$$f_0(z)=2c. \quad (15)$$

Thus finally we obtain the *common* solutions of the pair of functional equations (I) and (II), or (III) and (IV), *viz.*,

$$f_0(z), f_1(z), f_2(z), \ldots\ldots\ldots, f_n(z), \ldots\ldots\ldots$$

We may remark that the *common* solutions involve *two* and *only two* effective numerical parameters, these being the two arbitrary constants inherently present in the *arbitrary* solution $f_1(z)$ of the differential equation of the second order $T^{(1)}$. It is needless to point out that the constant value $(2c)$ of $f_0(z)$ is *not* an independent entity, but is rather dependent upon the two constants of $f_1(z)$ by virtue of (14) and (15).

It will be observed that the common solutions of (I) and (II) automatically satisfy the sequence of differential equations $\{T^{(n)}\}$*.

In the succeeding Article we propose to scrutinise in some detail the relationship that subsists among (III), (IV) and $T^{(n)}$.

Art. 3.—Starting with the two functional equations (III), (IV) and the differential equation $T^{(n)}$,

we shall combine them in three distinct pairs, *viz.*,

(III) and (IV), (III) and (A), (IV) and (A)

and study the legitimate inferences that can be drawn in each case.

CASE I.—First suppose that $f_n(z)$ satisfies (III) and (IV), (see Art. 1).

Then from (IV),

$$\tfrac{1}{2} \cdot \frac{d}{dz}\left\{zf_n(z) + \frac{1}{n} \cdot (z^2-1)f_n'(z)\right\} = f_{n+1}'(z)$$

$$= \frac{n+1}{z^2-1} \cdot \left\{zf_{n+1}(z) - \tfrac{1}{2}f_n(z)\right\}, \qquad \text{from (III)}$$

$$= \frac{n+1}{z^2-1} \cdot \left[z \cdot \tfrac{1}{2}\left\{zf_n(z) + \frac{1}{n} \cdot (z^2-1)f_n'(z)\right\} - \tfrac{1}{2}f_n(z)\right], \qquad \text{from (IV)}$$

which when simplified leads to (A).

---

* The differential equation $T^{(0)}$ being of the *degraded* form:

$$(1-z^2)f_0''(z) - zf'_0(z) = 0,$$

t is clear that $f_0(z) = \text{const.}$ is one of its solutions.

CASE II.—Next suppose that $f_n(z)$ satisfies (III) and (A). Then

$$\tfrac{1}{2}\cdot\left\{zf_{n-1}(z)+\frac{z^2-1}{n-1}\cdot f_{n-1}'(z)\right\}$$

$$=z\cdot\left\{zf_n(z)-\frac{1}{n}\cdot(z^2-1)f_n'(z)\right\}$$

$$+\frac{z^2-1}{n-1}\cdot\left\{zf_n'(z)+f_n(z)+\frac{1-z^2}{n}\cdot f_n''(z)-\frac{2z}{n}f_n'(z)\right\},$$

from (III)

$$=f_n(z),\qquad \text{on simplification by use of (A).}$$

$$\therefore\ zf_{n-1}(z)+\frac{z^2-1}{n-1}\cdot f'_{n-1}(z)=2f_n(z),$$

or,
$$zf_n(z)+\frac{1}{n}\cdot(z^2-1)f'_n(z)=2f_{n+1}(z),$$

which is no other than (IV).

CASE III.—Now suppose that $f_n(z)$ satisfies (IV) and (A). Then

$$2\cdot\left\{zf_{n+1}(z)-\frac{1}{n+1}\cdot(z^2-1)f_{n+1}'(z)\right\}$$

$$=z\cdot\left\{zf_n(z)+\frac{1}{n}\cdot(z^2-1)f_n'(z)\right\}$$

$$-\frac{1}{n+1}\cdot(z^2-1)\left\{zf'_n(z)+f_n(z)+\frac{1}{n}\cdot(z^2-1)f_n''(z)\right.$$

$$\left.+\frac{2z}{n}\cdot f_n'(z)\right\},\qquad \text{from (III)}$$

$$=f_n(z),\qquad \text{on simplification by aid of (A).}$$

$$\therefore\ zf_{n+1}(z)-\frac{1}{n+1}\cdot(z^2-1)f_{n+1}'(z)=\tfrac{1}{2}f_n(z),$$

or,
$$zf_n(z)-\frac{1}{n}\cdot(z^2-1)f_n'(z)=\tfrac{1}{2}f_{n-1}(z),$$

which is the same as (III).

Thus *the three equations* (III), (IV) and (A) *are so related that the combination of any two of them automatically leads to the third.*

Art. 4.—We shall close this topic with a brief reference to certain special solutions. It is directly verified that each of the three functions:

$$f_n(z)=\frac{1}{2^{n-1}}\cdot\sin(n\cos^{-1}z),\ \frac{1}{2^{n-1}}\cdot\cosh(n\cosh^{-1}z),\ \frac{1}{2^{n-1}}\sinh(n\cosh^{-1}z)\quad(16)$$

satisfies the two functional equations (I) and (II) and the differential equation (A). Besides, the function $V_n(z)$,* defined by

$$V_n(z) = -\frac{1}{2^{2n}} \cdot \frac{1}{z^n} \cdot F\left(\frac{n}{2}, \frac{n+1}{2}, 1+n; \frac{1}{z^2}\right), \quad (|z| > 1) \qquad (17)$$

and called "Tschebyscheff's Function of the Second Kind" is known to satisfy (I) and (A). So $V_n(z)$ must conform to the equation (II).

As remarked in the paper referred to in the foot-note, the general solution of (I), which is after all a functional equation of the second order, can be thrown into the form:†

$$f_n(z) = \alpha_n(z) \cdot \theta(z) + \beta_n(z) \cdot \phi(z), \qquad (18)$$

where $\alpha_n(z)$ and $\beta_n(z)$ are two particular solutions of (I) and $\theta(z)$, $\phi(z)$ are two *arbitrary* functions.

For obvious reasons, $\alpha_n(z)$ and $\beta_n(z)$ can at pleasure be replaced by *any two* of the functions $T_n(z)$, $V_n(z)$ and those marked (16).

---

* Refer to Bagchi and Chakravarty's paper, *viz.*, "*Note on Tschebyscheff function* $T_n(z)$ and *its associated equations*," where certain properties of the "so-called" Tschebyscheff's function of the second kind are discussed. (*Vide Journal of the Indian Math. Society*, 1950.)

† Throughout this paper, the parameter n is supposed to be a positive integer.

THERMAL EXPANSION OF CRYSTALS

Part VII. Barite

By S. S. Sharma

(From the Department of Physics, Indian Institute of Science, Bangalore)

Received March 3, 1951

(Communicated by Prof. R. S. Krishnan, F.A.SC.)

1. Introduction

Barite or heavy spar is a well-known mineral of which colourless and transparent big-sized crystals are easily obtainable. Hence it is not surprising that it has been a subject of investigation by various workers in different fields of study. Thus, R. S. Krishnan (1946) has studied its Raman spectrum with some thoroughness; while the temperature dependence of Raman frequencies and their width has been investigated by Narayanaswamy (1948). Amongst the directional properties, mention may be made of the elastic constant determinations of Voigt (1910) by static method and of Bergmann (1938) by dynamic method. Bridgman (1928) has measured the linear compressibilities of this crystal along the crystallographic axes. Results of magnetic susceptibility (K. S. Krishnan and others, 1933) and dielectric constant measurements (Rao, 1949) have also been reported in the literature. More recently the thermo-optic behaviour of this crystal has been studied in detail by Radhakrishnan (1951) in this laboratory.

In view of such diverse studies of the properties of this mineral, it is surprising to note that its thermal dilatation has not been studied so far. In I.C.T. (Vol. III, p. 44, 1928) is reported one value for the coefficient of linear expansion which appears to be misquoted. As an accurate knowledge of the directional dependence of thermal expansion is required for an understanding of the relation between thermal behaviour and crystal structure, the author has undertaken the measurements of thermal expansion of this crystal in different directions and the results of study are set forth in the present paper.

2. Procedure of the Experiment

Barite is an ionic crystal belonging to the bipyramidal class of the orthorhombic system. The relevant crystallographic data for identifying the faces are given by Groth (1908) according to whom the axial ratios are

$a:b:c=0{\cdot}8152:1:1{\cdot}3136$. The *c*-face (001) is a perfect cleavage plane. Cleavage along *b* (010) is also perfect, while along *m* (110) it is rather good. The symmetry of the crystal under investigation being orthorhombic, the three axes of the thermal ellipsoid coincide in direction with the crystallographic axes, and thus there are only three independent coefficients of expansion, *viz.*, α_{11}, α_{22} and α_{33}. Hence, for the purposes of the present investigation, three sets of spacers, in the form of right pyramids, with their altitudes coincident with the crystallographic axes, are needed. Two more sets of pyramids with their altitudes along (i) a direction equally inclined to the three axes and (ii) along a direction perpendicular to the natural cleavage *m*-face have been employed for verification and a check on the values previously determined.

The thermal expansion coefficient in an arbitrary direction is easily obtained by a transformation of axes to the concerned direction. The new set of axes X_1', X_2', X_3' are defined with respect to the old ones by the usual direction—cosine scheme:—

	X_1'	X_2'	X_3'
X_1	C_{11}	C_{12}	C_{13}
X_2	C_{21}	C_{22}	C_{23}
X_3	C_{31}	C_{32}	C_{33}

As usual α'_{33} indicates the constant in the arbitrary direction, which coincides with the X_3'-axis. The expression for α_{33}' is given by (Wooster, 1936)—

$$\alpha_{33}' = C_{13}^2\alpha_{11} + C_{23}^2\alpha_{22} + 2C_{13}C_{23}\alpha_{12} + 2C_{13}C_{33}\alpha_{13} + 2C_{23}C_{33}\alpha_{23} \qquad (1)$$

in the orthorhombic system α_{ij} $(i \neq j)$ vanish. The direction cosines for the arbitrary direction (i) are given by

$$C_{11} = C_{22} = C_{33} = \frac{1}{\sqrt{3}}$$

Hence we get

$$\alpha_{33}' = \tfrac{1}{3}\Sigma\,\alpha_{ii}. \qquad (2)$$

For the expansion perpendicular to the *m*-face, the expression (1) further simplifies

$$\alpha_{\perp m} = C_{13}^2\alpha_{11} + C_{23}^2\alpha_{22}. \qquad (3)$$

The specimen of the crystal of barite at the disposal of the author had its cleavage planes *c* and *m* perfectly well marked out. The axes were located with the help of ordinary polaroids. The *c*-axis was contained in the *m*-plane, while '*a*' and '*b*' in the *c*-plane. The latter were identified by the length of intercepts made by the *m*-plane with them.

3. Results and Their Discussion

The coefficients of thermal expansion, α_a, α_b, α_c along the three crystallographic axes *a*, *b* and *c* are entered in Tables I–III. The calculated values of the same from the interpolation formulæ are also put forth in the same tables.

Table I

Coefficient of linear expansion for barite parallel to the a-*axis*

$$\alpha_a = 0{\cdot}0_4 1362 + 0{\cdot}0_7 1298\, t + 0{\cdot}0_{10} 1192\, t^2$$

Temperature °C.	$\alpha_a \times 10^6$ observed	$\alpha_a \times 10^6$ calculated	Difference %
44·3	14·23	14·22	..
78·5	14·67	14·71	− ·3
111·2	15·24	15·21	+ ·2
142·5	15·83	15·71	+ ·7
175·6	16·26	16·26	..
210·6	16·76	16·88	− ·7
244·3	17·48	17·50	..
276·4	18·27	18·12	+ ·8
307·3	18·83	18·73	+ ·5
340·8	19·36	19·43	− ·4
377·1	20·21	20·21	..

Table II

Coefficient of linear expansion for barite parallel to the b-*axis*

$$\alpha_b = 0{\cdot}0_4 2395 + 0{\cdot}0_7 1256\, t + 0{\cdot}0_{10} 1368\, t^2$$

Temperature °C.	$\alpha_b \times 10^6$ observed	$\alpha_b \times 10^6$ calculated	Difference
42·6	24·58	24·51	+ ·3
74·5	24·98	24·96	..
105·6	25·43	25·43	..
136·1	25·86	25·91	− ·4
170·9	26·42	26·50	− ·3
209·6	27·18	27·1	..
247·0	28·01	27·89	+ ·4
283·5	28·68	28·61	+ ·2
319·1	29·29	29·35	− ·2
353·8	30·12	30·08	..
387·5	31·10	30·87	+ ·8

TABLE III

Coefficient of linear expansion for barite parallel to the c-axis

$$\alpha_c = 0{\cdot}0_4 1407 + 0{\cdot}0_7 1520\, t + 0{\cdot}0_{10} 1102\, t^2$$

Temperature °C.	$\alpha_c \times 10^6$ observed	$\alpha_c \times 10^6$ calculated	Difference
45·5	14·73	14·78	− ·4
70·8	15·09	15·20	− ·7
95·2	15·62	15·62	..
118·7	16·08	16·03	+ ·3
141·4	16·51	16·44	+ ·4
167·1	17·00	16·92	+ ·3
195·5	17·44	17·46	..
223·2	18·03	18·01	..
249·8	18·67	18·55	+ ·7
275·6	19·09	19·09	..
303·7	19·72	19·70	..
334·1	20·23	19·38	− ·8
363·6	20·97	21·05	− ·4

The values of $\alpha_{a,b,c}$, the coefficient of expansion along a direction equally inclined to the axes are entered in Table IV. The interpolation formula

$$\alpha_{a,b,c} = 0{\cdot}0_4 1720 + 0{\cdot}0_7 1369\, t + 0{\cdot}0_{10} 1204\, t^2$$

has been derived from the experimental values of α_a, α_b and α_c by employing the relation (2) given above. The calculated values of $\alpha_{a,b,c}$ from this formula are entered in the third column of this table. From a perusal of these values it can be seen that the agreement between the experimental and calculated values is quite satisfactory.

TABLE IV

Coefficient of expansion for barite in a direction equally inclined to the axes

Temperature °C.	$\alpha_{abc} \times 10^6$ (observed)	$\alpha_{abc} \times 10^6 = \frac{1}{3} \Sigma \alpha_{ii}$
48·4	17·91	17·89
79·2	18·31	18·36
109·0	18·81	18·84
138·0	19·28	19·31
166·1	19·77	19·81
196·7	20·36	20·36
229·7	20·94	20·98
261·6	21·63	21·61
292·6	22·24	22·24
322·6	22·89	22·87
351·9	23·41	23·51

The values of $\alpha_{\perp m}$ are entered in Table V.

TABLE V

Coefficient of expansion for barite perpendicular to m*-face*

$$\alpha = 0{\cdot}0_41770 + 0{\cdot}0_71254\,t + 0{\cdot}0_{10}1262\,t^2$$

Temperature °C.	$\alpha_{\perp m} \times 10^6$ observed	$\alpha_{\perp m} \times 10^6$ calculated	Difference %
43·4	18·28	18·27	..
75·1	18·84	18·71	+ ·7
105·7	19·28	19·17	+ ·6
135·5	19·72	19·63	+ ·5
164·6	20·07	20·10	− ·2
195·8	20·59	20·64	− ·3
228·8	21·23	21·23	..
260·8	21·94	21·83	+ ·5
291·8	22·55	22·43	+ ·5
321·9	23·04	23·04	..
355·0	23·62	23·74	− ·4

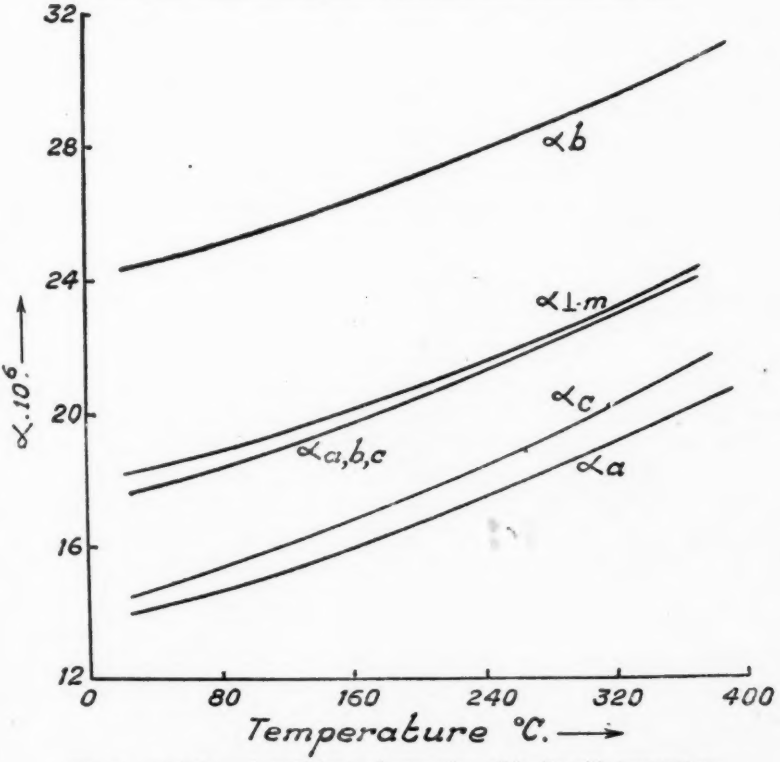

FIG. 1. Variation of coefficients of expansion of barite with temperature.

The variation of the various coefficients of expansion with temperature has been depicted by smooth curves in Fig. 1.

$\alpha_{\perp m}$ can also be evaluated from the observed values of α_a and α_b by employing relation (3) given above. Thus if θ be the angle between the normal to the *m*-plane and *a*-axis, the relation (3) reduces to

$$\alpha = \alpha_a \cos^2 \theta + \alpha_b \sin^2 \theta \qquad (4)$$

where $\theta = \tan^{-1} 0{\cdot}8152 = 39° 9'$.

For the sake of comparison the experimental values of $\alpha_{\perp m}$ are tabulated below along with those calculated from (4).

TABLE VI

Coefficient of expansion ($\times 10^6$) *perpendicular to* m-*face*

Temperatute °C.	0° C.	100° C.	200° C.	300° C.	400° C.
$\alpha_{\perp m}$ (observed)	17·70	19·08	20·71	22·60	24·74
$\alpha_{\perp m}$ (calculated) Equation (4)	17·74	19·14	20·80	22·72	24·89

Although there is a systematic deviation between these two sets of values, yet the discrepancy is not very marked and the agreement can be taken to be fairly satisfactory.

The values of the principal coefficients of expansion at 0° C. have been calculated and are given below:—

$$\alpha_a = 13{\cdot}62 \times 10^{-6}; \quad \alpha_b = 23{\cdot}95 \times 10^{-6}; \quad \alpha_c = 14{\cdot}07 \times 10^{-6}.$$

It is seen that the thermal anisotropy is maximum along the *b*-axis, while along the *a*- and *c*-axes the coefficients are nearly equal. The exact inequality can be represented by $\alpha_b > \alpha_c > \alpha_a$. It may be mentioned here that in this respect the thermal behaviour of barite is different from its optical behaviour. According to Groth (1908) the principal refractive indices are $n_a = 1{\cdot}6491$, $n_b = 1{\cdot}6381$ and $n_c = 1{\cdot}6369$. Thus in this case $n_a > n_b > n_c$. The optical and thermal ellipsoids are differently oriented in the crystal. But a survey of the literature shows that many other properties of barite, namely dielectric constant, magnetic susceptibility, linear compressibility, etc., exhibit anisotropy in the same sense as the coefficient of thermal expansion, *i.e.*, being maximum along the *b*-axis and minimum along the *a*-axis.

In conclusion, the author expresses his heart-felt thanks to Professor R. S. Krishnan for his constant interest in the work.

Summary

The paper describes the results of study of the thermal expansion of barite and its directional dependence. The principal coefficients of linear expansion along the crystallographic axes are given by

$$\alpha_a = 0{\cdot}0_41362 + 0{\cdot}0_71298\ t + 0{\cdot}0_{10}1192\ t^2$$

$$\alpha_b = 0{\cdot}0_42395 + 0{\cdot}0_71256\ t + 0{\cdot}0_{10}1368\ t^2$$

$$\alpha_c = 0{\cdot}0_41407 + 0{\cdot}0_71520\ t + 0{\cdot}0_{10}1102\ t^2.$$

References

Bergmann	..	*Ultrasonics*, 1938.
Bridgman	..	*Am. J. Sci.*, 1928, **15**, 292.
Groth	..	*Chem. Krystallographie, Zweiter Teil*, 1908, 388.
Krishnan, K. S. and others		*Phil. Trans.* 1933, **231 A**, 242.
Krishnan, R. S.	..	*Proc. Ind. Acad. Sci.*, 1946, **23**, 288.
Narayanaswamy, P. K.	..	*Ibid.*, 1948, **28**, 40.
Radhakrishnan, T.	..	*Ibid.*, 1951, **33**, 22.
Rao, D. A. A. S. N.	..	*Ibid.*, 1949, **30**, 82.
Voigt	..	*Lehrbuch der Krystalphysik*. 1910.
Wooster	..	*Crystal Physics*, 1936.

NOTE ON THE MUTUAL RELATION BETWEEN THE TWO KINDS OF TSCHEBYSCHEFF'S FUNCTIONS

By Hari Das Bagchi and Bhola Nath Mukherjee

Received January 11, 1950
(Communicated by Prof. B. S. Madhava Rau)

Introduction

The object of the present note is to trace the connecting link between the Tschebyscheff's function ("of the first kind"), *viz.*, $T_n(z)$ and the Tschebyscheff's function "of the second kind", *viz.*, $V_n(z)$ introduced in a paper by H. Bagchi and N. K. Chakravarty, published elsewhere.[1]

1. Defining the sequence of constants $\{c_{q,p}\}$ by the relation:

$$c_{q,p} \equiv \int_{-1}^{1} \frac{v^q T_p(v)\, dv}{(1-v^2)^{\frac{1}{2}}},$$

where $T_p(v)$ is Tschebyscheff's function of the first kind and the parameters p, q are *positive* integers, we note the relations[2]:

(i) $c_{q,p} = 0$, if $q < p$,

and (ii) $c_{q,p} = \frac{\pi}{2^{2p-1}}$ if $q = p$.

By aid of a suitable formula of reduction, one can easily substantiate the following additional properties:

(iii) $c_{q,p} = 0$, if $q > p$ and $q - p$ be an *odd* integer;

and (iv) $c_{q,p} = \frac{\pi}{2^{2(p+r)-1}} \cdot {}^{p+2r}C_r$, if $q > p$ and $q - p$ be an *even* integer $2r$.

In particular, we note the following special cases of (iv):—

$$c_{n+2,n} = \frac{\pi}{2^{2n+1}} \cdot \frac{n+2}{1!}; \qquad c_{n+4,n} = \frac{\pi}{2^{2n+3}} \cdot \frac{(n+3)(n+4)}{2!};$$

$$c_{n+6,n} = \frac{\pi}{2^{2n+5}} \cdot \frac{(n+4)(n+5)(n+6)}{3!}, \text{ and so on.}$$

2. Tschebyscheff's function $V_n(z)$ "of the second kind", has been defined by

$$V_n(z)=\frac{1}{2^{2n}}\cdot\left[\frac{1}{z^n}+\frac{n(n+1)}{4\cdot 1!\,(n+1)}\cdot\frac{1}{z^{n+2}}+\frac{n(n+1)(n+2)(n+3)}{4^2\cdot 2!\,(n+1)(n+2)}\cdot\frac{1}{z^{n+4}}\right.$$
$$\left.+\frac{n(n+1)(n+2)(n+3)(n+4)(n+5)}{4^3\cdot 3!\,(n+1)(n+2)(n+3)}\cdot\frac{1}{z^{n+6}}+\ldots.\right] \qquad (1)$$

where $|z|>1$.

Plainly the R.S.

$$=\frac{n}{2\pi}\cdot\left[\frac{1}{nz^n}\cdot\frac{\pi}{2^{2n-1}}+\frac{1}{(n+2)\,z^{n+2}}\cdot\frac{\pi}{2^{2n+1}}\cdot\frac{n+2}{\angle 1}+\frac{1}{(n+4)\,z^{n+4}}\cdot\frac{\pi}{2^{2n+3}}\right.$$
$$\left.\cdot\frac{(n+3)(n+4)}{\angle 2}+\frac{1}{(n+6)\,z^{n+6}}\cdot\frac{\pi}{2^{2n+5}}\cdot\frac{(n+4)(n+5)(n+6)}{\angle 3}+\ldots.\text{to }\infty\right]$$
$$=\frac{n}{2\pi}\cdot\left[\frac{1}{nz^n}\cdot c_{n,n}+\frac{1}{(n+2)\,z^{n+2}}\cdot c_{n+2,n}+\frac{1}{(n+4)\,z^{n+4}}\cdot c_{n+4,n}\right.$$
$$\left.+\frac{1}{(n+6)\,z^{n+6}}\cdot c_{n+6,n}+\ldots.\right], \text{ by Art. 1.}$$

Using the relation:

$$c_{q,n}=0, \text{ if } q\neq n \text{ and } q-n \text{ be odd,}$$

we can fill up the missing gaps in the sequence of terms in the above series and thus write

$$V_n(z)=\frac{n}{2\pi}\cdot\left[\frac{1}{z}\cdot c_{1,n}+\frac{1}{2z^2}\cdot c_{2,n}+\frac{1}{3z^3}\cdot c_{3,n}+\ldots.+\frac{1}{(n-1)\,z^{n-1}}\cdot c_{n-1,n}\right.$$
$$\left.+\frac{1}{nz^n}\cdot c_{n,n}+\frac{1}{(n+1)\,z^{n+1}}\cdot c_{n+1,n}+\frac{1}{(n+2)\,z^{n+2}}\cdot c_{n+2,n}+\ldots.\text{ to }\infty\right]$$
$$=\frac{n}{2\pi}\cdot\sum_{r=1}^{\infty}\frac{1}{rz^r}\cdot\int_{-1}^{}\frac{(v)^r T_n(v)}{(1-v^2)^{\frac{1}{2}}}\cdot dv, \qquad (|z|>1). \qquad (2)$$

Inasmuch as the series on the R.S. of the familiar equality:

$$-\log\left(1-\frac{v}{z}\right)=\sum_{r=1}^{r=\infty}\frac{1}{r}\cdot\left(\frac{v}{z}\right)^r, \ (-1<v<1, \ |z|>1) \qquad (3)$$

is absolutely and uniformly convergent for unrestricted variation of v in the domain $(-1, 1)$ and the multiplication by the *bounded* quantity,* *viz.*,

$$\frac{T_n(v)}{(1-v^2)^{\frac{1}{2}}} \tag{4}$$

does not affect the uniform convergence, we conclude on the strength of known lemmas of Analysis that the series (3), when multiplied by (4), must retain the property of uniform and absolute convergence so as to admit of term-by-term integration.

Consequently we obtain:

$$\sum_{r=1}^{r=n} \int_{-1}^{1} \frac{T_n(v)}{(1-v^2)^{\frac{1}{2}}} \cdot \left(\sum_{r=1}^{r=\infty} \frac{1}{r} \cdot \frac{v^r}{z^r} \right) dv = -\int_{-1}^{1} \frac{T_n(v)}{(1-v^2)^{\frac{1}{2}}} \cdot \log_e \left(1 - \frac{v}{z}\right) dv.$$

Hence by (2),

$$V_n(z) = -\frac{n}{2\pi} \cdot \int_{-1}^{1} \frac{T_n(v)}{(1-v^2)^{\frac{1}{2}}} \cdot \log_e \left(1 - \frac{v}{z}\right) dv, \quad (|z| > 1) \tag{5}$$

An equivalent formula is:

$$V_n(z) = -\frac{n}{2\pi} \cdot \int_{-1}^{1} \frac{T_n(v)}{(1-v^2)^{\frac{1}{2}}} \log(z-v)\, dv, \quad (|z| > 1) \tag{6}$$

(5) or (6) may be regarded as the analogue of Neumann's integral formula for $Q_n(z)$ in terms of the Legendre function of the first kind $P_n(z)$.

3. The legitimacy of differentiation (*w.r.t.* the parameter z) under the integral sign in the R.S. of (6) of the foregoing article being kept in view, we immediately deduce:

$$V_n'(z) = -\frac{n}{2\pi} \cdot \int_{-1}^{1} \frac{T_n(v)}{(z-v)(1-v^2)^{\frac{1}{2}}} dv. \tag{1}$$

Writing $T_n(v)$ in the form:

$$T_n(v) = T_n(z) - \{T_n(z) - T_n(v)\}$$

* Strictly speaking, the function (3) is bounded in the interval $(-1+\epsilon, 1-\epsilon)$, where $\epsilon > 0$. At either end-point $(-1$ or $1)$, $(\epsilon = 0)$, the function (3) becomes infinite and the definite integral (4) becomes *improper*. It can be proved by *a' priori reasoning* that this improper integral is uniformly convergent at each of the two end-points, so that the term-by-term integration is valid.

and substituting in (1), we get:

$$V_n'(z) = -\frac{n}{2\pi} \cdot T_n(z) \int_{-1}^{1} \frac{dv}{(z-v)(1-v^2)^{\frac{1}{2}}} - K, \tag{2}$$

where

$$K \equiv \int_{-1}^{1} \frac{T_n(z) - T_n(v)}{(z-v)(1-v^2)^{\frac{1}{2}}}\, dv \tag{3}$$

Since $T_n(v)$ is a polynomial of the type:

$$T_n(v) \equiv a_0 v^n + a_2 v^{n-2} + a_4 v^{n-4} + \ldots\ldots,$$

the quantity

$$\frac{T_n(z) - T_n(v)}{z - v}$$

is a polynomial of order $(n-1)$ in z, *viz.*,

$$a_1(v) \cdot z^{n-1} + a_2(v)\, z^{n-2} + a_3(v)\, z^{n-3} + \ldots\ldots,$$

the coefficients of the different powers of z being polynomials of order not greater than $n-1$ in v.

Hence (3) may be re-written as:

$$K = b_1 z^{n-1} + b_2 z^{n-2} + b_3 z^{n-3} + \ldots\ldots,$$

where

$$b_r = \int_{-1}^{1} \frac{a_r(v)}{\sqrt{1-v^2}}\, dv.$$

Now the definite integral, occurring in (2), *viz.*,

$$\int_{-1}^{1} \frac{dv}{(z-v)(1-v^2)^{\frac{1}{2}}},$$

when evaluated by the substitution $w = \left(\frac{1-v}{1+v}\right)^{\frac{1}{2}}$, is easily seen to be

$$\frac{\pi}{(z^2-1)^{\frac{1}{2}}}.$$

Hence the equation (2) may be presented in the form:

$$V_n'(z) = -\frac{n}{2} \cdot \frac{T_n(z)}{(z^2-1)^{\frac{1}{2}}} - R_{n-1}(z), \qquad (|z| > 1) \tag{5}$$

where $R_{n-1}(z)$ is a polynomial of order $(n-1)$ in z.

The relation (5) may be looked upon as the analogue of the corresponding relation between the two kinds of Legendre functions, *viz.*,

$$Q_n(z) = \tfrac{1}{2} P_n(z) \log \frac{z+1}{z-1} - W_{n-1}(z),$$

where $W_{n-1}(z)$[3] is a polynomial of order $n-1$.

ART. 4. We shall now close this topic with a short note on the *analytic continuation* of the function $V_n(z)$.

For obvious reasons the function $V_n(z)$, as defined by the negative power-series (1) of Art. 2, exists in the region, exterior to the unit-circle Σ, *viz.*, $|z| = 1$. But the domain of analytic existence of the function $V_n(z)$ as defined by (6) of Art. 2, is comparatively wider. For the line-integral

$$\int_{-1}^{1} \frac{T_n(v) \log (z-v)}{(1-v^2)^{\frac{1}{2}}}\, dv, \qquad (1)$$

(taken along the segment Λ of the real axis, intercepted between the end-points 1 and -1) is easily seen to represent a function of the parameter z (real or complex), analytic anywhere in the finite part of the plane *except at points on* Λ. In fact, the finite segment Λ $(-1, 1)$ is the "so-called" *Hermite's Section* for the line-integral (1) and is accordingly a *line of discontinuity* for the function of z, as defined by it. It follows automatically that the same rectilinear segment Λ counts as a line of discontinuity for the function $V_n(z)$, as defined by (6) of Art. 2. In other words, the function $V_n(z)$, as defined by (6) of Art. 2, exists at all interior points (of Σ), other than those situated on the diameter Λ. Thus the passage from (1) of Art. 2 to (6) of Art. 2 implicitly involves the process of analytic continuation of the function $V_n(z)$.

REFERENCES

1. H. Bagchi and N. K. Chakravarty — "On Tschebyscheff's function $T_n(z)$ and its associated equations," *Jour. Ind. Math. Soc.*, 1950, **14**, 35–42.
2. *loc cit.*
3. Hobson .. .. *Spherical and Ellipsoidal Harmonics*, 1931, Arts. 31, 34, 42, 43, 47.

SYNERESIS OF SODIUM OLEATE GELS IN ORGANIC SOLVENTS

Part I. Effect of area of gel-surface on the syneresis of sodium oleate gels in pinene

By Mata Prasad, F.A.Sc. and V. Sundaram

(From the Chemical Laboratories, The Institute of Science, Bombay)

Received July 20, 1950

Holmes and co-workers[1] have found that the syneresis of silica gels varies directly as the area of gel-surface exposed for syneresis. However, Ferguson and Applebey[2] find that syneresis in silica gels is independent of the surface exposed. Chapman and Buchanan[3] have observed that the syneresis of starch gels prepared in larger tubes is greater than that of the gels prepared in smaller tubes. It is evident that the study of the effect of surface on the syneresis of gels is important and has not so far received much attention. The present investigation deals with the study of this effect in the case of gels of sodium oleate in pinene.

Experimental Technique

The following series of experiments were carrried out to study the effect of surface area on the syneresis of sodium oleate gels in pinene.

Series A.—Three flat-bottomed dishes of diameters of (1) 4·3 cm., (2) 7·1 cm., (3) 9·8 cm., respectively, were used. It was so arranged that the amount of the gel in each dish was proportional to its surface area. The thickness of the gel layer was practically kept constant.

Series B.—Varying amounts of the gel were taken in the same dish of 4·3 cm. diameter.

Series C.—The same amount of the gel-forming solution was taken in each of the three dishes used in Series A.

For all the experiments a solution of 1% sodium oleate in pinene was prepared by dissolving the requisite amount of sodium oleate in pinene at 140° C., according to the method followed by Prasad and co-workers.[4]

For the experiments in Series A, approximately 5 c.c. of the solution were transferred to dish (1), 14 c.c. to dish (2) and 27 c.c. to dish (3) and then allowed to set in the dishes. For the experiments in Series B, approximately 5 c.c., 10 c.c., 15 c.c., 21 c.c., and 27 c.c. of the solution were transferred to dish (1) and allowed to set. For the experiments in series C, approximately, 27 c.c. of the solution were transferred to each of the three dishes and allowed to set. All the dishes were kept in a thermostat maintained

at $30° \pm 0{\cdot}1°$ C. In all the cases the amount of syneresis was measured three hours after the gels had set by the method followed by Prasad, Hattiangdi and Mathur.[4]

Results

The results obtained are given in Table I in which the following notations are used:

D diameter of the dish in cm.,

h thickness of the gel layer in cm.,

s specific surface in sq. cm. per c.c. $\left[\text{equal to } \frac{\pi D\,(h + D/2)}{\pi D^2 h/4}\right]$,

W weight of the gel in grams,

x amount of syneresis in grams,

Y percentage syneresis equal to $\frac{100\,x}{W}$.

TABLE I

Series	D	h	s	W	X	Y	Y′
	4·3	0·3521	6·609	4·356	1·196	27·46	..
A	7·1	0·3407	6·433	11·500	2·806	24·35	..
	9·8	0·3460	6·187	22·250	5·400	24·56	..
	4·3	0·3521	6·609	5·356	1·196	27·46	27·46
	4·3	0·6869	3·842	8·500	1·912	22·50	15·97
B	4·3	0·9924	2·946	13·284	2·088	17·00	12·25
	4·3	1·3980	2·360	17·306	2·150	12·43	9·81
	4·3	1·8520	2·011	22·920	2·481	10·82	8·36
	9·8	0·3460	6·187	22·25	5·400	24·56	24·56
C	7·1	0·6651	3·568	22·45	4·100	18·26	14·18
	4·3	1·8520	2·011	22·92	2·481	10·82	7·99

Discussion of Results

It is seen from the above table that (i) if the specific surface is constant, the percentage syneresis is also constant, provided, however, the thickness of the gel is small and is of the order of 0·35 cm. (*cf.*, Series A), (ii) the percentage syneresis depends upon the specific surface, being greater, greater the specific surface (*cf.*, Series B and C), and (iii) the amount of syneresis per unit surface depends upon the thickness of the gel, if it is small,

and is nearly independent of the thickness if it is large. The values of percentage syneresis (Y'), given in the last column of Table I, calculated on the basis of the specific surface, using the value of Y for the gel of the smallest thickness in the B and C Series, show that there is no direct proportionality between *s* and Y. This observation is in contradiction to the conclusions of Holmes and co-workers[1] which are not supported even by their own experimental results. It is clear that the syneresis of gels of fair thicknesses is not wholly determined by the specific surface; presumably there are other factors as well which influence it.

The effect of surface area exposed on the syneresis of these gels can be explained as follows:

The number and the size of micelles in a gel depend upon the concentration of the dispersed phase and the temperature to which the gel-forming solutions is allowed to cool. Now, at any temperature, if a fixed volume of a gel sets in vessels of increasing surface area, the number of the micelles at the surface and therefore the number of interfibrillary spaces on the surface of the gel will increase. Since the exudation of the syneretic liquid must take place ultimately through the interfibrillary spaces on the surface of the gel, the increase in the number of such spaces would facilitate the flow of the exuded liquid and hence the amount of the syneresis in the same gel in a given time would depend upon its surface. However, if the height of the gel is increased within small limits an increase in the amount of syneresis may be expected, on account of (i) the increased hydrostatic pressure exerted by the increased column of the gel and (ii) the possible decrease in the stability of the gel on increase in the thickness, provided the increased height does not alter the gel-structure or change the number and size of the fibrils present therein.

Summary

The effect of the area of gel surface exposed on the syneresis of sodium oleate gels in pinene has been determined. It is observed that syneresis is directly proportional to the specific surface per unit volume of the gel, provided the thickness of the gel is small, and nearly constant. When greater thicknesses of the gel are considered syneresis is slightly higher than the value calculated on the basis of the specific surface.

References

1. Holmes, Kaufmann and Nicholas .. *J. Am. Chem. Soc.*, 1919, **41**, 1932.
2. Ferguson and Applebey .. *Trans. Faraday Soc.*, 1930, **26**, 642.
3. Chapman and Buchanan .. *Iowa State Coll. J. Sci.*, 1930, **4**, 441.
4. Prasad, Hattiangdi and Mathur .. *Proc. Ind. Acad. Sci.*, 1945, **21 A**, 105.

REDUCTION PROCESSES AT THE DROPPING MERCURY ELECTRODE IN PULSATING FIELDS : THE NICKEL ION

By K. S. G. Doss, F.A.Sc. and A. Kalyanasundaram
(*Indian Institute of Sugar Technology, Kanpur*)

Received November 24, 1950

Introduction

Breyer and Gutman[1] have evolved a new and interesting technique for studying the electrode kinetics of the reversible depolarising processes taking place at a dropping mercury electrode by superimposing an alternating field. Systems involving the discharge of cadmium, thallium and zinc ions have been studied by them with an alternating field of 50 cycles per second. The discharge of lead ions has been studied by a similar technique by Doss and Agarwal[2] using the oscillograph for measuring the alternating current. They have extended the study to different frequencies of the field ranging from 12·5 to 600 cycles per second. The present paper reports the work on the discharge of nickel ions studied by a modified technique.

Experimental

The circuit diagram is given in Fig. 1. The source of alternating current is a B.S.R. oscillator capable of giving frequencies ranging from 0–16,000 cycles per second. 10 Volts from the oscillator is fed on to a potentiometric arrangement ACDB consisting of the resistances R_1, R_2 and R_3. This arrangement serves to give 45 mv. across R_2 which is superimposed on the dropping electrode along with a D.C. voltage obtained from a Cambridge pH potentiometer (with the galvanometer shorted off) used as a potential divider. The voltage output of the potentiometer across YZ can be varied at will, the resistance R_4 being 225 ohms per volt of D.C. voltage.

When the pulsating (A.C. superimposed on D.C.) potential is incident on the dropping electrode, a pulsating current is produced. Our present interest is to measure the A.C. component of the pulsating current. For measuring this, the arrangement used is as follows:—A valve amplifier system (Fig. 1) working on the non-linear portion of the characteristic curves of the valves, partially rectifies and amplifies any incident alternating potential. This amplified current is incident on a Leeds and Northrup galvanometer (period: 14·5 sec.; resistance: 1,182 ohms; shunt: 99 ohms). The tapping key K connects the amplifier system to the potential drop across R_3 in the

rest position P, and to that across R_5 when the key is depressed to the position P_2. First, the resistance R_3 is reduced to zero, thereby making the input to the amplifier system zero. The current passing through the galvanometer under these conditions is compensated by the potentiometer. Then the resistance R_3 is increased to 3 ohms, thereby making the input to the

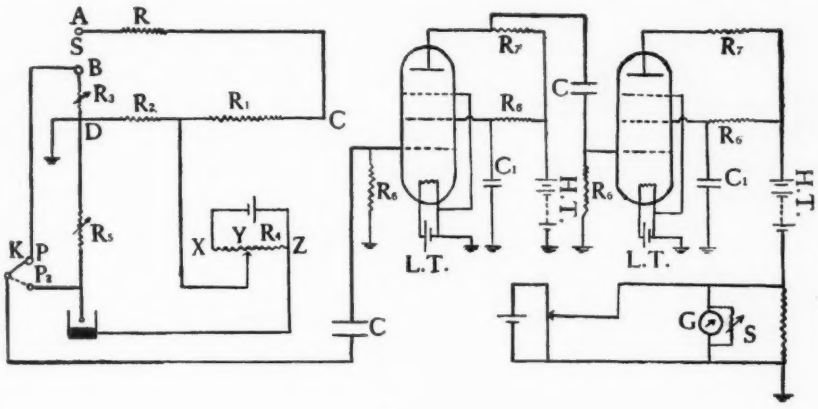

FIG. 1

$R = 600\,\Omega$	$C = 0{\cdot}25\,\mu F$
$R_1 = 13{,}000\,\Omega$	$C_1 = 0{\cdot}1\,\mu F$
$R_2 = 58\,\Omega$	L.T. = 1·5 V
$R_3 = 0{\cdot}3\,\Omega$	H.T. = 45 V
$R_4 = 225\,\Omega$ per volt of D.C.	$S = 99\,\Omega$
$R_5 = 0-2{,}500\,\Omega$ (according to the current)	$R_6 = 5\,M\Omega$
	$R_7 = 1\,M\Omega$

amplifier equal to 2·3 mv. The galvanometer gets deflected. The reading on the galvanometer scale is noted. Any current passing through the dropping electrode passes through the resistance R_5. The potential drop thus obtained across R_5 is applied to the amplifier system by depressing the tapping key to the position P_2. In this position R_5 is adjusted so as to give the same deflection of the galvanometer as was obtained for a potential of 2·3 mv. (*i.e.*, in the position P, of the tapping key). By knowing the value of the resistance R_5, the current can be calculated. The condenser serves to filter off the D.C. component of the pulsating current.

This arrangement for measuring the current has the following advantages: (1) The measurement is not affected by any changes with time in the characteristics of the amplifying system. (2) It is also unaffected by

the variation of the characteristics of the amplifier with the change in frequency of the A.C.

The dropping electrode has the following characteristics:

m: 0·69 mg./sec.

t : 5·3 sec. in 0·1 M — KCl_{aq}. in open circuit.

The experiment is first performed with IM KCl containing no other dischargeable ions. Hydrogen, obtained from a Kipp after purification by passing through mercuric chloride, lead acetate and distilled water is passed in the solution for 15 minutes to remove traces of oxygen. The A.C. passing through the dropping electrode at the different D.C. potentials are measured as explained above and the results are represented in Fig. 2. The experiments are carried out at different frequencies of the A.C.

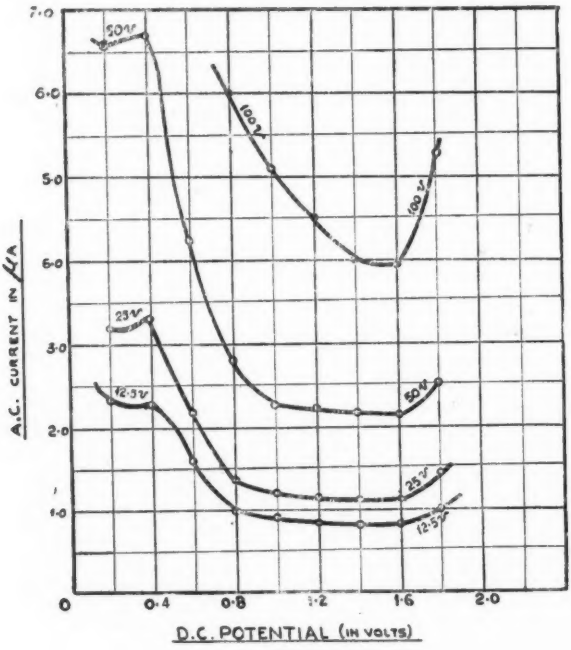

FIG. 2

The experiment is repeated with IM KCl containing $3·27 \times 10^{-3}$ M nickel ions (in the form of nickel chloride) and the results are represented in Fig. 3.

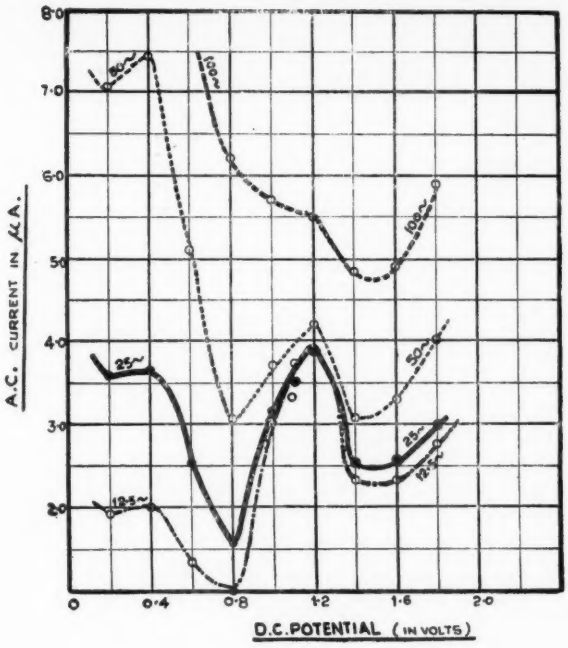

FIG. 3

Fig. 4 represents the polarographic curve of nickel obtained with the same dropping electrode.

DISCUSSION

Our results confirm in general the observation made by Breyer and Gutman[1] that a maximum in the alternating current occurs nearly at the half-wave potential of the system in question. Fig. 4 shows the polarographic curve from which the half-wave potential comes out to be at about 1·1 volt. The alternating current maximum from Fig. 3, comes out to 1·2 volt, which is nearly the half-wave potential. The D.C. potential at which the a.c. maximum occurs is independent of the frequency of the a.c. field. This is in agreement with the observation made by Doss and Agarwal (*loc. cit.*). There is one important difference, however, between these curves and the curve obtained by Doss and Agarwal. Whereas the value for the alternating current at the maximum in their system was nearly independent of the frequency, with nickel it is found that there is a large stepping up of the a.c. current as the frequency is changed from 50 to 100 cycles per second. This difference in behaviour can be explained as follows:

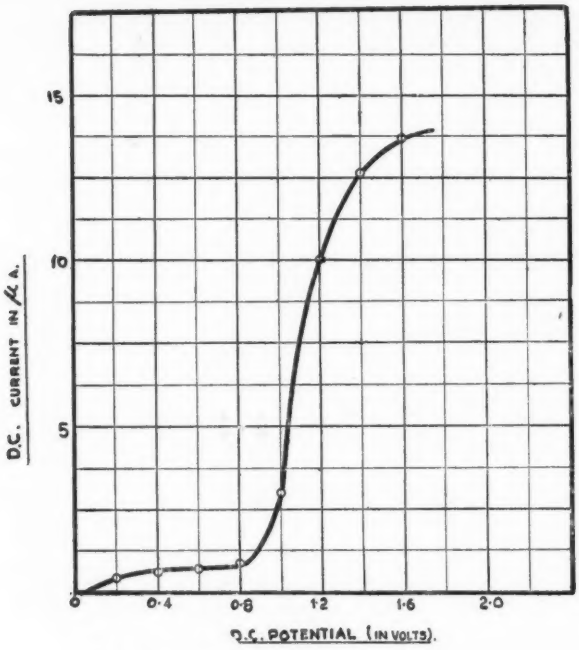

FIG. 4. *Polarographic current : Nickel*

The dropping mercury electrode in contact with the solution of the electrolyte presents an electric double layer which behaves like a capacity in absence of any reducing ions. The increase in the a.c. current with increase in frequency (Fig. 2) is due to the diminution of the capacitative impedance. The effect of the presence of the reducible ions is equivalent to shorting the electric double layer capacity by a resistance, or more generally by an impedance consisting of a resistance and a capacity in parallel the value of which decreases with the increase in the intensity of the discharge of the reducible ions. The effect of this is to reduce the overall capacitative impedance. At the half-wave potential of the reducible ions the discharge is maximum and hence there is a maximum in the alternating current. It appears that in the system dealt with by Doss and Agarwal, this maximum capacitative impedance becomes a very small fraction of the total impedance of the system so that the change of frequency has no marked effect on the overall impedance of the system at the a.c. maximum. With the system dealt with in this paper, however, the minimum capacitative impedance is yet comparable with the total impedance of the system and

hence an increase in the frequency has a marked effect on the value of the a.c. current at the half-wave potential.

Breyer and Gutman have worked out a quantitative theory to explain the form of the curves. One of the assumptions that they have started is that the alternating current at any instant would be equal to the polarographic current corresponding to the potential incident on the electrode at that instant. We have worked out the theoretical curve relating the a.c. current with the d.c. voltage on the basis of the above assumption alone. This is shown in Fig. 5 (Curve I). The experimentally observed curve (Curve II) is given in the same figure for comparison. The above assumption of Breyer

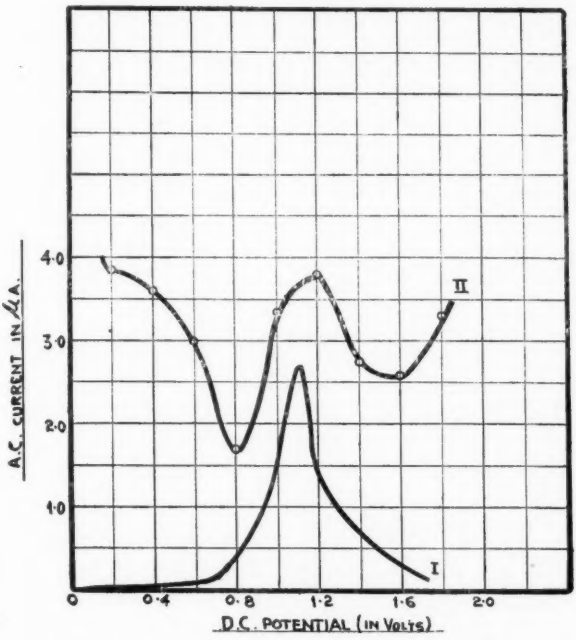

FIG. 5. *I. Theoretical Curve.* *II. Experimental Curve.*

and Gutman approaches nearest to the experiment at near the half-wave potential for this system at the frequencies of 12·5 and 25 cycles per second. At other frequencies and potentials, however, there are large deviations, the experimental values being much higher than the theoretical values. This divergence is to be traced to the fact that the measured polarographic current is an average figure whereas the a.c. current is caused by the

comparatively instantaneous changes in the current when the potentials are altered quickly.

A quantitative treatment of the observed phenomena appears to be possible only after more detailed and extensive experimental data on such systems become available.

The authors wish to thank Prof. J. M. Saha, Director, Indian Institute of Sugar Technology, Kanpur, for his kind interest in the work. The authors are grateful to the Uttar Pradesh Scientific Research Committee for a grant which made this work possible.

Summary

A method has been described for measuring small alternating currents. This has been applied for studying the a.c. currents induced in a dropping mercury electrode system containing nickel ions when subjected to a pulsating field at different frequencies of the field. This system has revealed interesting features which are different from the systems investigated by the previous workers.

References

1. Breyer and Gutman .. *Faraday Soc. Discussion*, 1947, No. 1, 19.
2. Doss and Agarwal .. *Proc. Ind. Acad. Sci.*, 1951, 33, 66.

SYNERESIS OF SODIUM OLEATE GELS IN ORGANIC SOLVENTS

Part II. Effect of time on the syneresis of sodium oleate gels in pinene and xylene

By Mata Prasad, F.A.Sc. and V. Sundaram

(From the Chemical Laboratories, The Institute of Science, Bombay)

Received September 13, 1950

The effect of time on the syneresis of silica gels seems to have been first studied by Okatov[1] who suggested that syneresis is a good measure of the maturity of these gels. Ferguson and Applebey[2] have observed that in the initial stages, the velocity of syneresis of silica gel follows an autocatalytic curve. Prasad, Hattiangdi and Mathur[3] have studied the kinetics of the syneresis of sodium oleate gels in pinene and have found that, for the interval of time studied, syneresis follows a relation similar to the imbibition of liquids. The present paper deals with the investigation of syneresis of sodium oleate gels in pinene and in xylene carried out over an extended period of seven days.

Experimental

It has been pointed out in the previous paper[4] that syneresis varies with the surface of the gel. Hence in these investigations test-tubes of the same internal diameter, 1·70 cm., were used throughout. Gels containing 0·10 g. of sodium oleate in 10 c.c. of each solvent were used for the measurement of syneresis. The gels in pinene were prepared in the manner described in Part I.[4] The gels in xylene were prepared in a similar manner by preparing the solution of sodium oleate in xylene at 130° C. All the gels were kept in a thermostat maintained at 30° ± 0·1° C. The amount of syneresis was measured by the method of Prasad and co-workers[3] at different known intervals of time after the gels had just set.

Results

The results obtained are given in the following table in which the following notations have been used:

t = time after the gel had set, and

X = the amount of syneresis in grams.

TABLE I

t in hrs.	Gels in pinene		Gels in xylene	
	X	$K_m \times 10^6$	X	$K_m \times 10^6$
1	0·600	20·250	1·703	60·900
2	0·795	13·550	1·798	32·370
3	0·923	10·630	1·844	22·200
5	1·088	7·577	1·861	13·460
7	1·165	5·823	1·872	9·658
18	1·317	2·587	..	..
24	1·374	2·031	1·945	2·941
48	1·485	1·107	2·008	1·529
144	..	..	2·074	0·529
168	1·729	0·375	2·090	0·457

DISCUSSION OF RESULTS

It is seen from Table I that the gels in xylene synerise more rapidly than those in pinene. The graphs of the amount of syneresis against time are smooth rising curves (Fig. 1) and are not S-shaped as observed by Ferguson and Applebey.[2] This shows that the process of syneresis of sodium oleate gels both in pinene and in xylene is not autocatalytic.

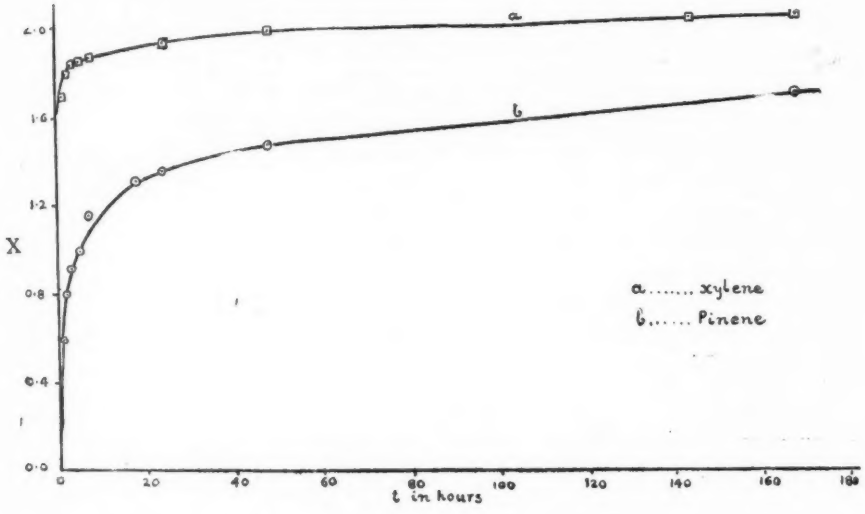

FIG. 1

Lipatov[5] has observed that the velocity of syneresis in geranin gels follows the law of first order reaction. Prasad and co-workers[3] have found

that the unimolecular constants (K_m) calculated for different intervals of time in a given series are not constant but decrease as the time interval is increased, thereby showing that the law of unimolecular reaction is not obeyed in this case. They have also noticed that the graphs obtained by plotting X/t against K_m are straight lines, showing that the relation $X/t = KK_m + C$, where K and C are constants, is followed in this case. Similar results have been obtained in this investigation on the syneresis of sodium oleate gels in pinene as well as in xylene (*cf.*, Columns 3 and 5, Table I).

Prasad and co-workers[3] have found that the relation $X^n = kt$ in which n and k are constants, holds good in the case of sodium oleate gels in pinene. Hence the graphs of log X against log t have been drawn, using the data given in Table I, and the plotted points appear to lie on a pair of intersecting straight lines (*cf.*, Fig. 2). This indicates that (i) two stages are involved in the process of syneresis of gels in xylene and pinene and (ii) the velocity of the second stage is much smaller than that of the first. The existence of the second stage is noticed only after a sufficient amount of the syneretic liquid has been exuded out of the gel. This happens much earlier in xylene than in pinene. The existence of the second stage has not been observed by Prasad and co-workers[3] since the period for which they measured the syneresis was not sufficiently long to bring out this phenomenon.

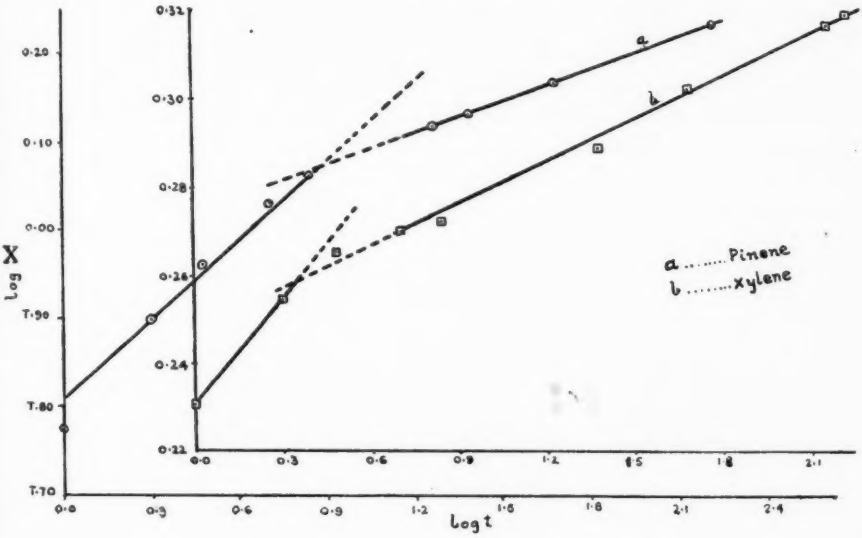

FIG. 2

The above observations can be explained as follows: When a solution of sodium oleate in pinene or xylene is cooled, at some temperature the soap goes over to the colloidal state due to super-saturation. On further cooling, the colloidal particles of the soap agglomerate in the form of fibrils. During the formation of colloidal particles and their agglomeration, a part of the dispersion medium gets attached to the particles due to solvation. This part of the dispersion medium corresponds to the bound liquid in gels (*cf.*, Hardy[6]). The fibrils form the gel structure enclosing the remaining dispersion medium (called free liquid by Hardy) within the interfibrillary spaces. When the gel starts synerising either due to the collapse of the structure as a whole or due to the fibrils coming closer to each other, the liquid within the interfibrillary spaces gets exuded; this corresponds to the initial stage of rapid syneresis. Subsequently, due to the structural changes taking place in the gel, probably a breakdown of the individual fibrils themselves, some of the bound liquid is also exuded; this corresponds to the second stage of syneresis. Since the structural changes in a gel take place comparatively slowly, the second stage of syneresis is a slow process.

One of the authors (V. S.) is grateful to the authorities of the University of Bombay for awarding him a University Research Studentship during the progress of this investigation.

Summary

The effect of time on the syneresis of sodium oleate gels in pinene and xylene has been investigated. The graphs of synereticum against time are smooth rising curves and are not S-shaped as is the case with silica gels. The rate of syneresis is large in the initial period and falls off continuously with time. The progress of syneresis does not follow the law of first order reaction observed in the case of geranin gels. The plots of log X against log t for the gels in both the solvents give, in each case, a pair of intersecting straight lines indicating the existence of two different processes of syneresis. An explanation has been advanced for this behaviour.

References

1. Okatov .. *Zhur. Prikladnvi khim*; 1929, **2**, 21.
2. Ferguson and Applebey .. *Trans. Faraday Soc.*, 1930, **26**, 642.
3. Prasad, Hattiangdi and Mathur .. *Proc. Ind. Acad. Sci.*, 1945, **21 A**, 105.
4. ——— and Sundaram .. Part I Communicated for publication.
5. Lipatov .. *Kolloid Z.*, 1927, **43**, 396.
——— and Korobova .. *Z. anorg. allgem. Chem.*, 1930, **194**, 377.
6. Hardy .. *Kolloid Z.*, 1928, **46**, 268.

THE THEORY OF OPTICAL ACTIVITY OF CRYSTALS

II. Calculation of the Rotatory Power of $NaClO_3$ and $NaBrO_3$

BY G. N. RAMACHANDRAN, F.A.SC.

(From the Department of Physics, Indian Institute of Science, Bangalore 3)

Received February 5, 1951

1. INTRODUCTION

IN Part I, an account of the general theory has been given together with an example of the application of the theory to a hypothetical structure. In this part, it is proposed to apply the theory to calculate the values of rotatory power for two crystals of the cubic system, $NaClO_3$ and $NaBrO_3$. We shall retain the symbols used in Part I.

Both $NaClO_3$ and $NaBrO_3$ belong to the tetartohedral (T) class of the cubic system. Their structures have been determined by several workers (Dickinson and Goodhue, 1921; Kolkmeijer, Bijeovet and Karsson, 1921; Kiby, 1923; Zachariasen, 1929). All of them agree in placing the structure in the space-group T^4-P2_13 and in giving the number of molecules per unit cell as 4. The co-ordinates of the different atoms in one of the enantiomers are as follows with respect to a right-system of co-ordinates:

4 Na	uuu;	$\frac{1}{2}+u, \frac{1}{2}-u, \bar{u}$; $\bar{u}, \frac{1}{2}+u, \frac{1}{2}-u$; $\frac{1}{2}-u, \bar{u}, \frac{1}{2}+u$
4 Cl (4 Br)	vvv;	etc.
12 O	xyz;	$\frac{1}{2}+x, \frac{1}{2}-y, z$; $\bar{x}, \frac{1}{2}+y, \frac{1}{2}-z$; $\frac{1}{2}-x, \bar{y}, \frac{1}{2}+z$
	yzx;	etc.
	zxy;	etc.

The different workers, however, give slightly different values for u, v, x, y, z. Of the various measurements, that of Zachariasen is the most accurate; but he has studied only $NaClO_3$. Consequently, Zachariasen's data are taken for this crystal, *viz.*, $u=0{\cdot}064$, $v=0{\cdot}417$, $x=0{\cdot}303$, $y=0{\cdot}592$, $z=0{\cdot}500$ and lattice parameter $a=6{\cdot}57$ Å. The data of Dickinson and Goodhue for $NaClO_3$ agree closely with this and therefore their measurements for $NaBrO_3$ have been used for our calculations. They are: $u=0{\cdot}09$, $v=0{\cdot}41$, $x=0{\cdot}30$, $y=0{\cdot}60$, $z=0{\cdot}47$ and $a=6{\cdot}71$ Å.

The unit cell is shown in Fig. 1, where the four O_3 groups have been labelled 1, 2, 3, 4 respectively. We shall first consider sodium chlorate.

2. Calculation of the Polarisabilities

From the refractive index ($n_D = 1 \cdot 514$) of sodium chlorate, the molar refraction of the compound is calculated to be $R = 12 \cdot 8$. Now, it is well known that the positive ion has a low molar refraction (Fajans and Joos, 1924; Pauling, 1927). For Na, this is of the order of 0·5. As regards ClO_3^- ion, no values are available in the literature for the contributions of Cl and O atoms separately. However, the following table for ions of the type AO_3 taken from the data in Fajans and Joos' paper is helpful. The table shows that the atom A in the ion AO_3 always has a small molar refraction.

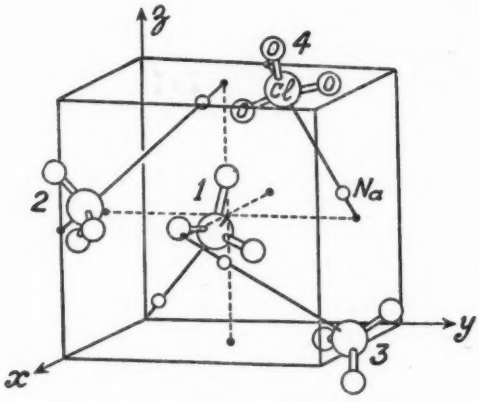

Fig. 1. Unit Cell of Sodium Chlorate

Table I

Ion	R_O	R_A
CO_3^{--} ..	4·08	0·03
SiO_3^{--} ..	4·42	0·10
NO_3^- ..	3·66	0·02
SO_3^{--} ...	3·65	0·05
ClO_4^- ..	3·32	0·04

We may therefore choose similarly a low value 0·05 for the Cl atom in ClO_3. Thus, we may take $R_{Na} = 0 \cdot 45$, $R_{Cl} = 0 \cdot 05$, $R_O = 4 \cdot 1$, which lead to the value 12·8 for $NaClO_3$. This set of values is reasonable, since the value 4·1 for R_O is about the mean value found in different ions of the type AO_3, although

larger than in ClO_4. Using Heaviside units, we have the polarisability $\alpha = 3\,R/N$, where N is the Avogadro number. Thus,

$$\alpha_{Na} = 0{\cdot}22,\ \alpha_{Cl} = 0{\cdot}025,\ \alpha_O = 2{\cdot}03 \times 10^{-23} \qquad (1)$$

Now, in calculating the interactions of the different atoms in the structure, we may take the ClO_3 group as a unit. Further, since the Cl atoms contribute only about $\frac{1}{2}\%$ of the polarisability of this group, we may neglect them for convenience and consider only the O_3 group. Calculations from the structure show that the O_3 group is an equilateral triangle, the O—O distance (d) being 2·38 Å. Consequently, we may calculate the principal polarisabilities of this group, using the method of Bragg (1924). If $\alpha_\perp$ and $\alpha_{||}$ are respectively the polarisabilities normal to the plane of the O_3 group and for directions in the plane, then their values are calculated to be

$$\alpha_\perp = 4{\cdot}92 \times 10^{-23},\ \alpha_{||} = 7{\cdot}14 \times 10^{-23}. \qquad (2)$$

In the $NaClO_3$ structure, therefore, we may replace each set of 3 oxygen atoms by a single anisotropic group having the above components for the polarisability and situated at the centre of gravity of the triangle. The co-ordinates of the centres of gravity of the four O_3 groups, as well as the orientation of the normals to their planes, are indicated below:

1. w, w, w	2. $\frac{1}{2}+w, \frac{1}{2}-w, \bar{w}$	3. $\bar{w}, \frac{1}{2}+w, \frac{1}{2}-w$	4. $\frac{1}{2}-w, \bar{w}, \frac{1}{2}+w$
[111]	[1 $\bar{1}$ 1]	[1 1 $\bar{1}$]	[$\bar{1}$ 1 1]

with $w = 0{\cdot}465$.

We shall make a further simplification by neglecting all the sodium atoms also (since these contribute only about 4% to the total polarisability). Thus, for the purpose of our calculations, we are left with four anisotropic O_3 groups, 1 to 4, per unit cell.

It is convenient to take Ox, Oy, Oz along the cubic axes of the crystal. Since the O_3 groups all have their normals along one or the other of the four [[111]] axes, their polarisabilities α_{ij} referred to cubic axes can be described by two parameters $A = (\alpha_\perp + 2\alpha_{||})/3$ and $B = (\alpha_\perp - \alpha_{||})/3$. The components of the polarisability tensor for the four O_3 groups are given below:

Type 1			Type 2			Type 3			Type 4			
A	B	B	A	−B	−B	A	−B	B	A	B	−B	
B	A	B	−B	A	B	−B	A	−B	B	A	−B	(4)
B	B	A	−B	B	A	B	−B	A	−B	−B	A	

Clearly, $A = 6{\cdot}40 \times 10^{-23}$ and $B = -0{\cdot}74 \times 10^{-23}$ (5)

3. Calculation of the Interaction of Neighbours

In the structure, each O_3 group is surrounded by twelve others (similar to the 12 next nearest neighbours of the same type in the NaCl structure). The co-ordinates of the twelve neighbours of group 1 are shown in Table II, taking that particular group as origin. These are divided into three sets of four each, all the groups in one set having the same orientation. Similar tables can be prepared for the neighbours of groups 2, 3 and 4.

Table II

Neighbours of O_3 Group 1

Type	Co-ordinates
2	0·50, −0·43, 0·07; −0·50, −0·43, 0·07; 0·50, 0·57, 0·07; −0·50, 0·57, 0·07
3	0·07, 0·50, −0·43; 0·07, −0·50, −0·43; 0·07, 0·50, 0·57; 0·07, −0·50, 0·57
4	−0·43, 0·07, 0·50; −0·43, 0·07, −0·50; 0·57, 0·07, 0·50; 0·57, 0·07, −0·50

Now consider light having its electric vector parallel to Ox being propagated along the positive z-axis. Then the phase of the wave at an atom (x, y, z) is exp. $(-kaz)$, since x, y, z are expressed as fractions of the unit cell dimension a. Since none of the components of the polarisability tensor are zero, all the four types of O_3 groups will have components of electric moment along Ox, Oy and Oz. Taking these into account, the induced fields F_x, F_y, F_z are calculated at each group. Each of these three components would produce an additional moment parallel to all three axes. In this way, the final induced moments μ_x and μ_y (taking into account the influence of neighbours) is calculated for all the four groups in the unit cell. Adding them up, we obtain

$$\sum_1^4 \mu_{rx} = \left[25{\cdot}6 \times 10^{-23} - \frac{2}{\pi a^3}(0{\cdot}115\,A^2 + 0{\cdot}928\,AB + 8{\cdot}50\,B^2)\right] \left(E_x + \frac{P_x}{3}\right) \quad (6)$$

$$\sum_1^4 \mu_{ry} = i\,\frac{2}{\pi a^3}(0{\cdot}100\,AB + 3{\cdot}096\,B^2)\,ka\left(E_x + \frac{P_x}{3}\right) \quad (7)$$

Since λ in the medium is λ_0/n, where $\lambda_0 = 5{\cdot}893 \times 10^{-5}$ for the sodium D line, we have

$$P_x = 0{\cdot}9042\,(E_x + P_x/3); \quad P_y = 0{\cdot}685 \times 10^{-5} n\,(E_x + P_x/3) \quad (8)$$

From these, we obtain $n = 1{\cdot}514$ and $g/n = 9{\cdot}806 \times 10^{-6}$. Thus

$$\rho = \frac{\pi}{\lambda_0} \cdot \frac{g}{n} = 30°{\cdot}0 \text{ per cm.}$$

This compares well with the experimentally observed value of 31°·3. The excellent agreement between the two must be considered to be fortuitous. In fact, small changes in the parameters used would lead to an appreciable alteration in the value of the rotatory power. It is however interesting to note that the theory gives the right order of magnitude.

4. Rotatory Power of Sodium Chlorate in the Ultra-Violet

Calculations similar to the above can readily be made in the ultra-violet if the polarisabilities of the individual atoms are known. Unfortunately, all studies on molar refraction, etc., have been confined to a single wavelength, *viz.*, the D line and no data are available in the literature for the ultra-violet. However, an approximate estimate can be made as shown below. We consider the wavelength $\lambda_0 = 2573$ Å for which the rotatory power of $NaClO_3$ has been measured by Rose (1909). The refractive index for this wavelength is 1·585, so that the calculated molar refraction is 14·3. This has to be divided into the separate contributions of Na, Cl and O. It would not be correct to divide them in the same ratio as for λ 5893 since oxygen would have a smaller dispersion than the other two. A reasonable estimate is as follows:

$$R_{Na} = 1{\cdot}0,\ R_{Cl} = 0{\cdot}1,\ R_O = 4{\cdot}4.$$

Naturally, there is a certain amount of uncertainty in these estimates, but they enable us to calculate the order of magnitude of ρ. These lead to $\alpha_{Na} = 0{\cdot}50$, $\alpha_{Cl} = 0{\cdot}05$ and $\alpha_O = 2{\cdot}17$, $\times 10^{-23}$, from which we have

$$\alpha_{\parallel} = 2{\cdot}59,\ \alpha_{\perp} = 1{\cdot}73,\ A = 6{\cdot}91,\ B = -0{\cdot}86,\ \times 10^{-23}.$$

Substituting in equations (6) and (7) and making the calculations just as for λ 5893, one finds $\rho = 226°$, as compared with the value 147°·3 found experimentally. It is interesting to note that the order of magnitude is correct.

5. Calculations for Sodium Bromate

Rose (*loc. cit.*) has also measured the optical rotatory power of $NaBrO_3$ from 4000 to 7500 Å and we give below his data for two wavelengths near the upper and lower limits:

λ_0	n	ρ
7188	1·610	13°·9
4047	1·643	72°·0

Taking 7,188 first, the value of R_{NaBrO3} is calculated to be 15·0. There appear to be no data in the literature as to the individual values of R_{Br} and R_O in the bromate ion. We, therefore, make the following estimates.

$$R_{Na} = 0{\cdot}5,\ R_{Br} = 0{\cdot}7,\ R_O = 4{\cdot}6.$$

R_{Na} is the same as in $NaClO_3$. Since Br is a much larger atom than Cl, we have taken R_{Br} to be fairly large. R_O has a value larger than in ClO_3, but we cannot reduce it further without abnormally increasing R_{Br}. The above values lead to $\alpha_{\parallel} = 2{\cdot}66 \times 10^{-23}$ and $\alpha_{\perp} = 1{\cdot}86 \times 10^{-23}$ for the O_3 group. If we take the co-ordinates of Dickinson and Goodhue (*loc. cit.*) for the atoms in the unit cell of $NaBrO_3$, the O—O distance is 2·51 Å and the centres of gravity of the O_3 groups occur at w, w, w, etc., where $w = 0{\cdot}46$. This value of w is close to the value 0·465 in $NaClO_3$, so that we may take the latter here also and no detailed calculations need be made, except to put in the appropriate values of the polarisabilities in equations (6) and (7). As in $NaClO_3$, here also we neglect the effects of Na and Br, as they contribute only about 8% to the total polarisability. It is calculated that $A = 7{\cdot}18 \times 10^{-23}$ and $B = -0{\cdot}80 \times 10^{-23}$ and with these ρ is found to be equal to 22·1° for λ 7188.

Taking 4047, R_{NaBrO3} is 15·65. Obviously, the molar refraction of oxygen would vary very little from λ 7188 to λ 4047, since oxygen has a dispersion frequency in the remote ultra-violet. Further, most of the dispersion must be due to bromine, since $NaBrO_3$ absorbs light completely below 4000 Å, while $NaClO_3$ does so only below 2200 Å. Hence, we estimate the contributions of the different atoms as follows:

$$R_{Na} = 0{\cdot}6,\ R_{Br} = 1{\cdot}0,\ R_O = 4{\cdot}65.$$

Thus $A = 7{\cdot}21 \times 10^{-23}$, $B = -0{\cdot}80 \times 10^{-23}$ and ρ is calculated to be 71° for λ 4047.

6. Discussion of the Results

The calculated and the experimental values of ρ for the two crystals are shown in Table III.

Table III

$NaClO_3$			$NaBrO_3$		
	ρ(th)	ρ(exp.)		ρ(th)	ρ(exp.)
5893	30°·0	31°·3	7188	22°·1	13°·9
2573	226°	147°·3	4047	71°·0	72°·0

The agreement should be considered satisfactory, since the values for the polarisabilities are not very accurate.

The structure of $NaClO_3$ can be considered to be derived from the NaCl structure by a slight distortion in which both the anions and cations

are displaced parallel to the body diagonals. If the O_3 groups considered above occupy exactly the points of a face centred lattice (like the Cl's in NaCl), *i.e.*, $w = 0 \cdot 50$ in (3), then the rotation vanishes. In fact, it can be shown that the ensemble of O_3 groups then form a structure belonging to the space-group T_h^6—P*a*3, which should not exhibit optical activity. It is the small deviation from this arrangement that is responsible for the optical activity of both sodium chlorate and sodium bromate.

If the O_3 groups are taken to be isotropic, then clearly $B = 0$ and the right-hand side of equation (7) will be zero, so that $\rho = 0$. Thus, anisotropy of the individual groups is essential for optical activity to be present, as was mentioned in Part I.

We have calculated the anisotropy of the individual groups from theory in this paper. This is not quite necessary. In fact, they can be obtained from data on the scattering of light by solutions of the crystals. Studies of this type have been made for ions like SO_4 and NO_3 (Sweitzer, 1927), but not for ClO_3 or BrO_3 ions. If reliable experimental values are available for the anisotropy of the cations, then a more accurate comparison will be possible between theory and experiment.

Summary

The theory of optical activity outlined in Part I has been applied to the cases of $NaClO_3$ and $NaBrO_3$. The calculated values for the rotatory power agree reasonably well with measurements previously reported.

References

1. Bragg .. *Proc. Roy. Soc.* 1924, **105A**, 370.
2. Dickinson and Goodhue .. *J. Am. Chem. Soc.*, 1921, **43**, 2045.
3. Fajans and Joos .. *Z. f. Phys.*, 1924, **23**, 1.
4. Kiby .. *Ibid.*, 1923, **17**, 213.
5. Kolkmeijer, Bijeovet and Karsson .. *Proc. Amst.*, 1921, **23**, 644.
6. Pauling .. *Proc. Roy. Soc.*, 1927, **114A**, 191.
7. Rose .. *Diss. Gött.*, 1909.
8. Sweitzer .. *J. Phys. Chem.*, 1927, **31**, 1150.
9. Zachariasen .. *Z. Krist.*, 1929, **71**, 517.

REDUCTION PROCESSES AT THE DROPPING MERCURY ELECTRODE IN PULSATING FIELDS : THE LEAD ION

By A. Kalyanasundaram

(*Indian Institute of Sugar Technology, Kanpur*)

Received January 24, 1951

(Communicated by Prof. K. S. Gururaja Doss, F.A.SC.)

Introduction

Doss and Agarwal[1] have studied the discharge of the lead ions at the dropping mercury electrode by extending Breyer and Gutman's[2] technique to different frequencies of the A.C. field ranging from 12·5 to 600 cycles per second using the oscillograph for measuring the alternating current. Doss and Kalyanasundaram[3] have studied the discharge of the nickel ions by a modified technique. The present paper deals with the application of this technique to study the behaviour of lead ions.

Experimental

The circuit diagram is given in Fig. 1. The source of A.C. is a B.S.R. oscillator capable of giving frequencies ranging from 0–16,000 cycles per second. 10 Volts from the oscillator is fed on to a potentiometric arrangement consisting of resistances R, R_1, R_2, and R_3. This arrangement serves to give 45 mv. across R_2 which is superimposed on the dropping mercury electrode along with a D.C. voltage obtained from a Cambridge pH potentiometer (with the galvanometer shorted off) used as a potential divider. The A.C. component of the pulsating current is obtained after filtering off the D.C. across a condenser. This is measured by means of a two-stage amplification system consisting of 1 LD 5 valves.[3] R_5 is adjusted such that the potential drop across this gives the same deflection as that of the potential drop across R_3. Thus the A.C. current passing through the dropping electrode can be calculated from a knowledge of the resistance R_5. The frequency of the oscillator is maintained constant at the desired value making use of the Du Mont 208 B oscillograph.

The dropping mercury electrodes have the following characteristics:—

	Dropping electrode I (Fig. 3)	Dropping electrode II (Fig. 4)
m. (mg./sec.)	0·69	0·33
t in sec. in M KCl-aq; Open circuit	5·3	3·6

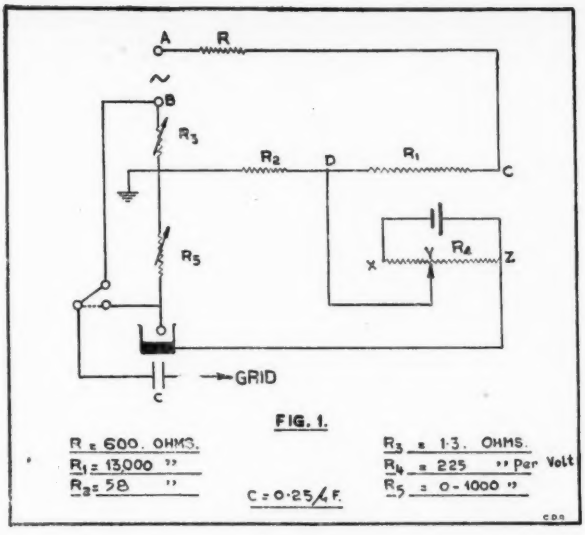
A
R
B
R3
R2
D
R1
C
R5
R4
X
Y
Z
GRID
C
FIG. 1.
R = 600. OHMS.
R1 = 13,000 "
R2 = 58 "
C = 0·25 μF.
R3 = 1·3. OHMS.
R4 = 225 " Per Volt
R5 = 0-1000 "

FIG. 1

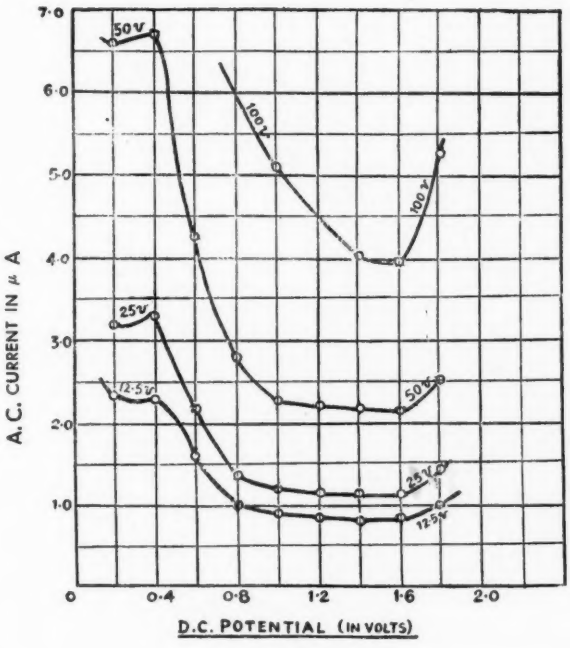
7·0
6·0
5·0
4·0
3·0
2·0
1·0
0
0·4
0·8
1·2
1·6
2·0
A. C. CURRENT IN μ A
D.C. POTENTIAL (IN VOLTS)
50 V
100 V
25 V
12·5 V

FIG. 2

The experiment is first performed with 1 M KCl containing no other dischargeable ions. Hydrogen of high purity is obtained electrolytically in the usual manner but with an auxiliary cathode helping in 'cleaning up' the residual oxygen diffusion.[4] This is passed into the solution for about fifteen minutes to remove the traces of oxygen present. The A.C. passing through the dropping electrode at the different D.C. potentials are measured. The experiments are carried out at different frequencies of A.C. and are represented in Fig. 2.

Figs. 3 and 4 represent the results obtained with 1 M KCl containing 2×10^{-3} M lead ions (in the form of lead nitrate).

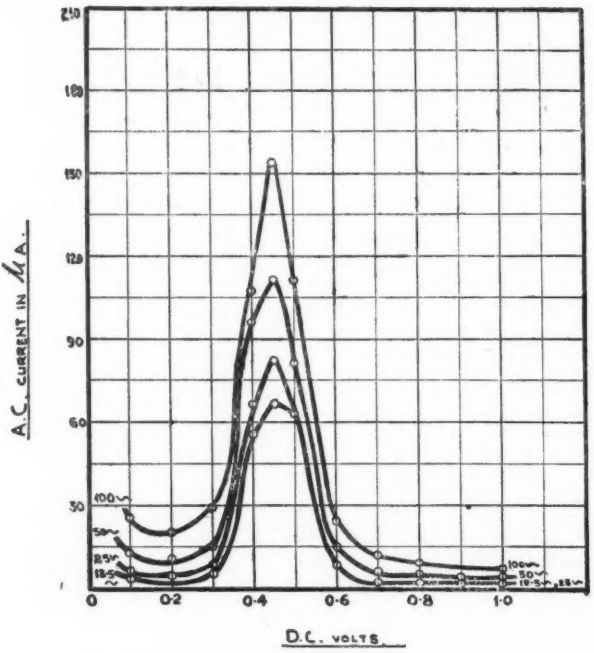

FIG. 3. Behaviour of lead ion in pulsating fields

Fig. 5 represents the polarographic curve of lead obtained with dropping electrode I.

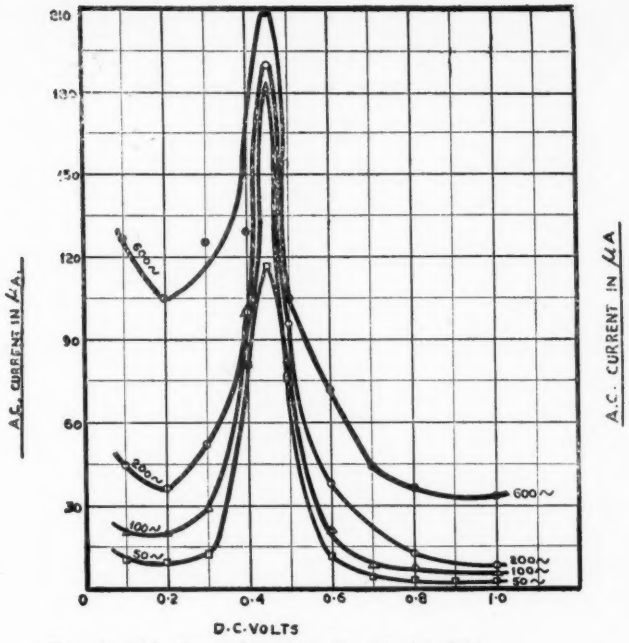

FIG. 4. Behaviour of lead ion in pulsating field

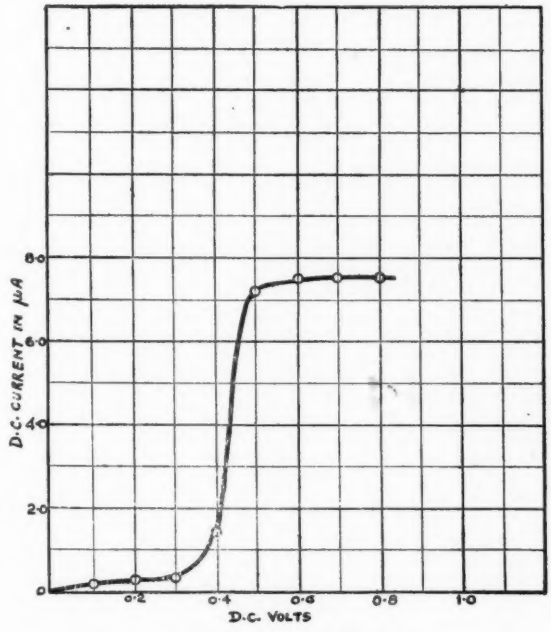

FIG. 5. Polarographic curve for lead

Discussion

The A.C. current–D.C. potential curves in the system containing the indifferent electrolyte only.—

An examination of Fig. 2 shows that the A.C. current starts with a high value at 0·4 V, falls rapidly upto 0·8 V, remains more or less constant upto 1·6 V and thereafter begins to rise. The first fall of A.C. current in the D.C. voltage interval of 0·4 V to 0·8 V coincides approximately with the region in which the electrocapillary maximum occurs. It is well known that the capacity of the electric double layer on the positive side of the electrocapillary maximum is much higher than on the negative side. From this point of view, it is of interest to calculate the capacity of the electric double layer from the observed alternating current values. There are complications arising out of the facts that an average current is measured and also that the size of the drop itself is changing with time. The relationship between the observed average alternating current and the capacity of the electric double layer can be formulated as follows:—The capacitative impedance due to the electric double layer at the mercury drop can be put as equal to K_1ct, where c represents the capacity of the electric double layer in farads/sq.cm. and $K_1 t$ is the area of the mercury drop at time t. If R is the external resistance in ohms, the average current as registered in the measuring equipment will be

$$i_{av} = \frac{\int_0^{t_{max.}} \frac{E}{\left[R^2 + \frac{1}{(k_1 ct^{2/3})^2}\right]^{\frac{1}{2}}} dt}{t}.$$

Making rough calculations, on the basis of the above formula, taking R to be negligible we get for the capacities of electric double layer at 0·4 V and 1·2 V (with reference to N.C.E.) at 50 cycles/sec., the values of 67 and 26/μF respectively. These values are high as compared with the values of 49/μF and 22/μF per sq.cm. respectively as given by Philpot.[5] These high values may be partly due to the fact that the mercury drop is growing all the time during the measurement or it may be an artefact of some sort. The results however generally indicate the large changes in the capacities of the electric double layer near the electrocapillary maximum. The difference cannot be due to the fact that the effect of resistive impedance is neglected. For, the fact that the current gets nearly doubled as one passes from 25 to 50 cycles both at 0·8 V and 1·2 V shows that the existing impedance is mainly capacitative in character and the resistive part is comparatively

negligible. The later rise in the curves beyond 1·6 V is perhaps to be connected with some reductive process coming into play.

The A.C. current-D.C. potential curves in the system containing 0·002 *M lead in MKCl.—*

The observations of Breyer and Gutman that A.C. current maximum occurs at nearly the half-wave potential is confirmed by the present system as well. It is to be seen that the magnitude of the maximum goes on increasing with the frequency of A.C. even upto 600 cycles/second. This behaviour is different from that of nickel reported earlier[3] as well as from even that of lead itself as measured by Doss and Agarwal[2] using the oscillograph. With nickel, even at a frequency of 100 cycles/second, the maximum has disappeared. With lead, in the oscillographic mode of measurement, at 600 cycles/second, the maximum is of a negligible magnitude. Further, the magnitude of the A.C. by this method is much lower than that obtained in the present work.

The above facts can be understood by a detailed consideration of the phenomenon. This can be discussed from two points of view, *viz.*, the molecular kinetic and secondly, the electrical equivalent of the dropping mercury electrode. The molecular kinetic point of view may first be taken up. At low D.C. voltages, say, of the order of 0·2 V there is no discharge of lead ions and hence the system is behaving like a perfectly polarizable electrode. The capacity of the dropping electrode is small, its impedance large and hence the resultant A.C. current is small. As the half-wave potential is reached, the system becomes imperfectly polarizable due to the reduction of the lead ions. There are three important factors to be considered in this connection: the electrode process, *viz.*, the discharge of lead ions and dissolution of lead from the lead amalgam at the surface of the mercury drop, the diffusion processes building up the diffusion layers both on the solution side and in the mercury drop and thirdly, the external resistance of the system. It may be pointed out that the diffusion processes are more or less similar in all the systems studied, as the diffusion coefficients are oft he same order of magnitude. This would not therefore, bring about material differences in the behaviour of the different systems. The main cause of the differences in behaviour appears to be the rate of the electrode processes which may vary several thousand fold in the different systems. For instance, thallium has a rate constant of 1·5 units (moles per sq.cm. per second per mol. per c.c.) whereas zinc, with KNO_3 as indifferent electrolyte, has the value of $4{\cdot}3 \times 10^{-3}$.[6] Apart from the Randles technique which gives an elegant way of determining the rate constants, a qualitative idea of the same

can be had from the slope of the polarographic curves taken under similar conditions. A high slope indicates a fast reaction. When the A.C. is incident at the half wave potential, there will be a tendency for the electrode process to keep in pace with the pulsating field. The result will be a pulsating current. As has already been pointed out,[3] the A.C. component of the current cannot be predicted quantitatively from the polarographic curve. This is seen clearly from Fig. 6 wherein the theoretical A.C. current-

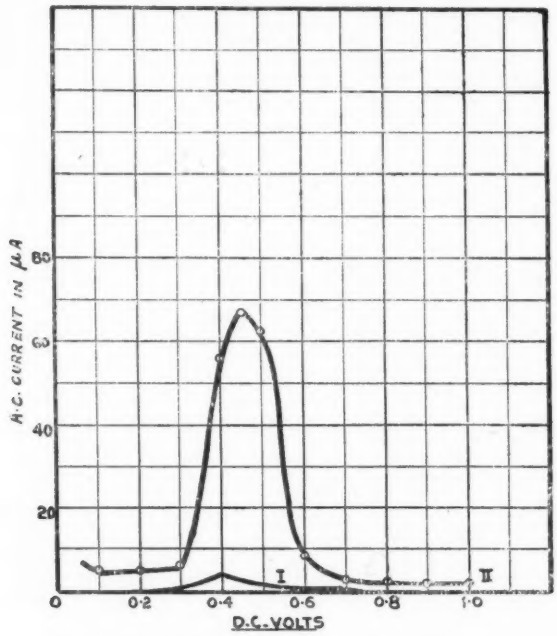

FIG. 6. Theoretical and experimental curve

D.C. voltage curve (Curve I, Fig. 6) worked out from the polarographic curve (Fig. 5) and the experimental curve at 12·5 cycles (Curve II, Fig. 6) are given. The observed A.C. current at the half-wave potential is much higher than that predicted on the basis of the polarographic curve. Further, this difference is much more at higher frequencies of A.C. The magnitude of the fluctuations in the current due to the fluctuating field would depend on the rapidity with which the electrode process would respond to the fluctuations. With a rapid electrode reaction as in the case of lead, the electrode reaction follows easily the fluctuations in the potential and hence large maxima are observed even at as high frequencies as 600 cycles/second.

Nickel, on the other hand, represents a slow electrode process. The Randles' technique has not yet been applied to a system involving nickel. But the rate of electrode process can be judged from the slope of the polarographic curve at the half-wave potential. According to the theory of absolute reaction rates,[7] the rate of the cathodic electrode process should fall exponentially with the fall in the cathodic potentials. This explains the quick rise of the polarographic wave near the half-wave potential. But the actual slope should depend on the free energy of activation for the particular electrode reaction. The slope would therefore be smaller for slow reactions and larger for fast reactions. The low slope of the polarographic wave for nickel indicates that it is a slow reaction. With nickel, therefore, the A.C. maximum disappears at a much lower frequency of the A.C., *viz.*, 100 cycles/second, at which the system behaves as if the nickel ions are absent and the solution contains only the indifferent electrolyte.

It is to be noted, however, that the response of the electrode reaction is dependent on the resistive impedance of the system as it would affect the movement of electrons taking part in the electrode processes. A high external resistance would bring down the maximum of the A.C. current and would lower the frequency at which the A.C. maximum would disappear. This phenomenon has perhaps a correspondence with the lowering of the slope of the polarographic curve at the half-wave potential with the increase in the external resistance. With slow reactions as the external resistance would have a greater effect, a pronounced A.C. maximum can be obtained only by having very low external resistances. With nickel (a slow electrode reaction), for instance, even at a circuit resistance of 600 ohms, the maximum has disappeared at 100 cycles per second whereas with lead with over 1,000 ohms[1] as circuit resistance the maximum is perceptible even at 600 cycles per second. In the present work, the persistance of a large maximum with lead even at 600 cycles is due to the very low circuit resistance (200 ohms) used in the present mode of measurement. A detailed investigation of the effect of external resistance will be published shortly.

It is to be pointed out that the difference between the current at the A.C. maximum and the corresponding current for the indifferent electrolyte at the same D.C. potential (Figs. 2 and 3) is a semi-quantitative measure of the amount of electrode process in which the lead ions are involved. It is to be seen that this difference is small at low frequencies, increases at higher frequencies, reaches a maximum and again becomes small at higher frequencies. The frequency at which the maximum difference is observed appears to be a measure of the rapidity of the electrode reaction if the

resistance of the circuit is constant. It is of interest to consider the possibility of determining the rate constant by these measurements suitably modified so as to avoid the complications arising from the changes due to the growing drop, the large amplitude of the applied A.C. potential as well as the average nature of the A.C. current measured.

Whatever has been discussed above can be pictured in terms of the electrical equivalent. The large rise in the A.C. current at the half-wave potential is a result of diminution in the impedance of the dropping electrode system. This can be pictured as brought about by two parallel shunts, *i.e.*, a resistance and a capacity to the electric double layer at the mercury-solution interface. The capacity shunt would have a high impedance for a slow reaction as in the case of nickel whereas it would have a low impedance in the case of lead. This would completely explain the observed frequency dependance. It is of interest to examine how the capacity shunt corresponding to the electrode reaction would get affected by changes in frequency.

Grateful thanks are due to Prof. K. S. G. Doss, D.Sc., F.R.I.C., F.Inst.P., F.A.Sc., Professor of Chemistry, Indian Institute of Sugar Technology, Kanpur, for his valuable guidance and discussions. Thanks are also due to Prof. J. M. Saha, M.Sc., Director, Indian Institute of Sugar Technology, Kanpur, for his kind interest and to the Uttar Pradesh Scientific Research Committee for a grant which made this work possible.

Summary

The discharge of the lead ions at the dropping mercury electrode has been studied by the Breyer and Gutman technique at different frequencies. This system has revealed interesting features which are different from the systems investigated by others. The results have been interpreted taking into account the kinetics of discharge of the lead ion at the electrode.

References

1. Doss and Agarwal .. *Proc. Ind. Acad. Sci.*, 1951, January Number.
2. Breyer and Gutman .. *Faraday Soc. Discussion*, 1947, No. 1, 19.
3. Doss and Kalyanasundaram *Proc. Ind. Acad. Sci.*, 1951, **33**, 298.
4. Clark .. *The Determination of Hydrogen Ions*, 353.
5. Philpot .. *Phil. Mag.*, 1932 (7), **13**, 775.
6. Randles .. *Faraday Soc. Discussion*, 1947, No. 1, 11 (Details of data by private communication).
7. Glasstone, Laidler and Eyring *The Theory of Rate Processes.*

288-51—Printed at The Bangalore Press, Bangalore City, by G. Srinivasa Rao, Superintendent and Published by The Indian Academy of Sciences, Bangalore